



Universidad
de Huelva

Pion and kaon parton distributions from their light- front wave functions

Chang Lei,
Khépani Raya,
Craig D. Roberts,
José Rodríguez-Quintero,

...

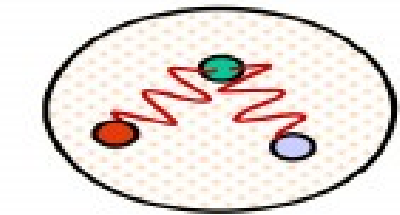


Perceiving the Emergence of Hadron Mass through AMBER@CERN: March 30, 2020.

Hadron Physics. General Motivation.

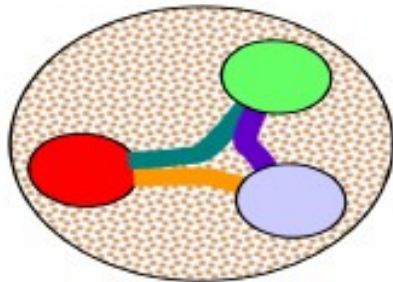


The QCD Holy Grail: the understanding of hadrons in terms of its elementary excitations; namely, quarks and gluons!



High

pQCD



3q-core

$\pi, \rho, \omega \dots$



3q-core+MB-cloud

Low

Confinement

Colored bound states have never been seen to exist as particles in nature

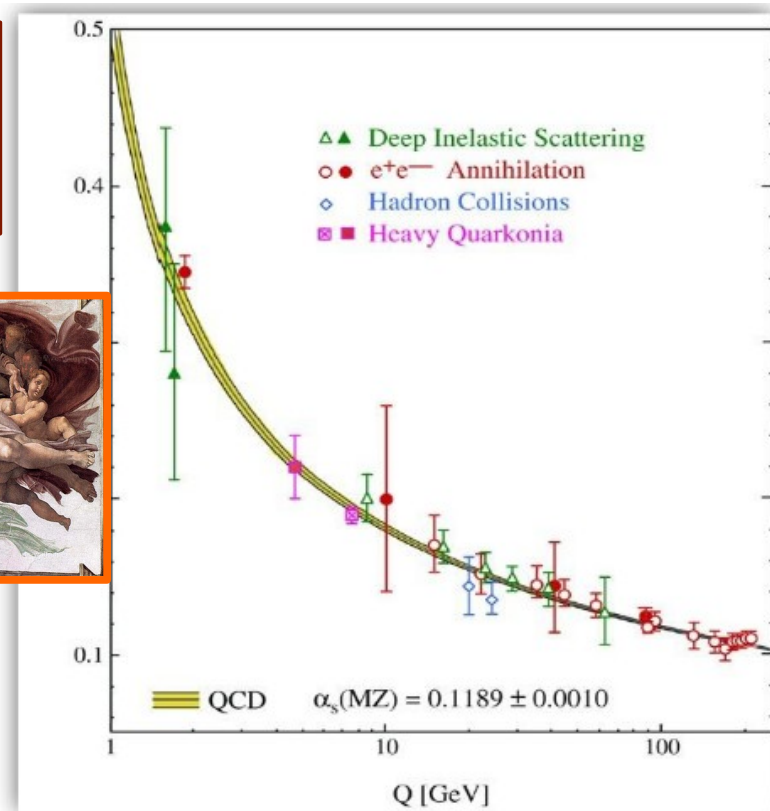
Q^2

What happens down here?



DCSB

Chiral symmetry appears dynamically violated in the Hadron spectrum



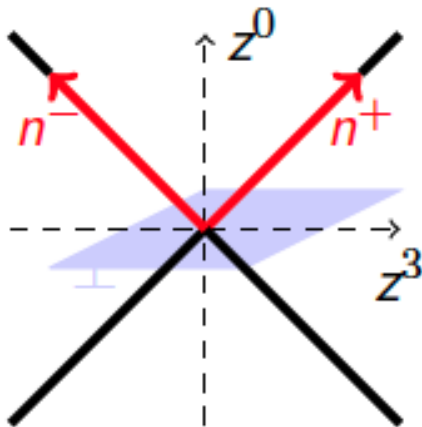
Emergent phenomena playing a dominant role in the real world dominated by the IR dynamics of QCD.

Antecedents:

GPD definition:

$$H_{\pi}^q(x, \xi, t) = \frac{1}{2} \int \frac{dz^-}{2\pi} e^{ixP^+z^-} \left\langle \pi, P + \frac{\Delta}{2} \left| \bar{q} \left(-\frac{z}{2} \right) \gamma^+ q \left(\frac{z}{2} \right) \right| \pi, P - \frac{\Delta}{2} \right\rangle_{\substack{z^+=0 \\ z_{\perp}=0}}$$

with $t = \Delta^2$ and $\xi = -\Delta^+ / (2P^+)$.



References

Muller et al., Fortchr. Phys. **42**, 101 (1994)
 Radyushkin, Phys. Lett. **B380**, 417 (1996)
 Ji, Phys. Rev. Lett. **78**, 610 (1997)

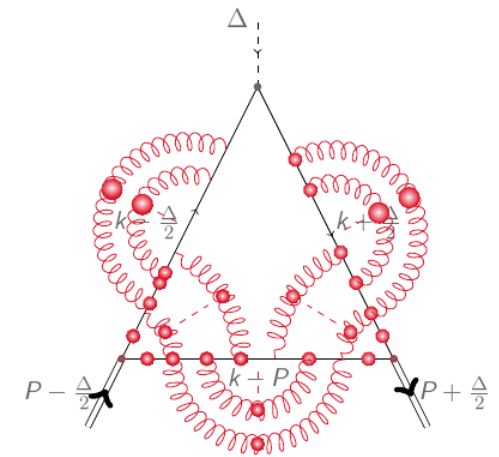
- From **isospin symmetry**, all the information about pion GPD is encoded in $H_{\pi^+}^u$ and $H_{\pi^+}^d$.

- Further constraint from **charge conjugation**:

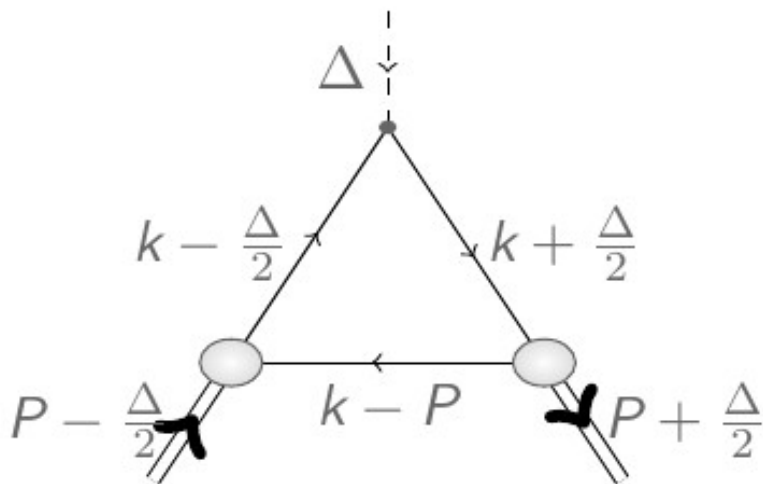
$$H_{\pi^+}^u(x, \xi, t) = -H_{\pi^+}^d(-x, \xi, t).$$

Antecedents:

GPDs in the Schwinger-Dyson and Bethe-Salpeter approach



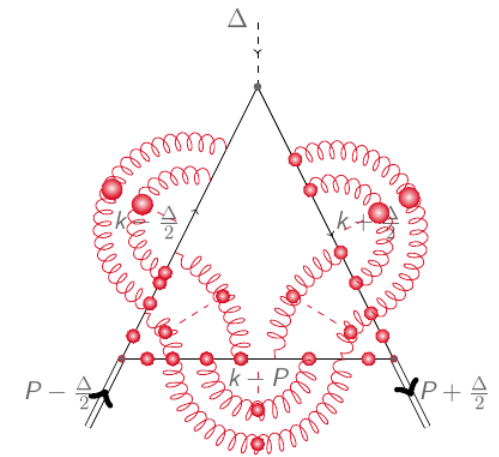
$$\langle X^m \rangle^q = \frac{1}{2(P^+)^{n+1}} \left\langle \pi, P + \frac{\Delta}{2} \left| \bar{q}(0) \gamma^+ (i \overleftrightarrow{D}^+)^m q(0) \right| \pi, P - \frac{\Delta}{2} \right\rangle$$



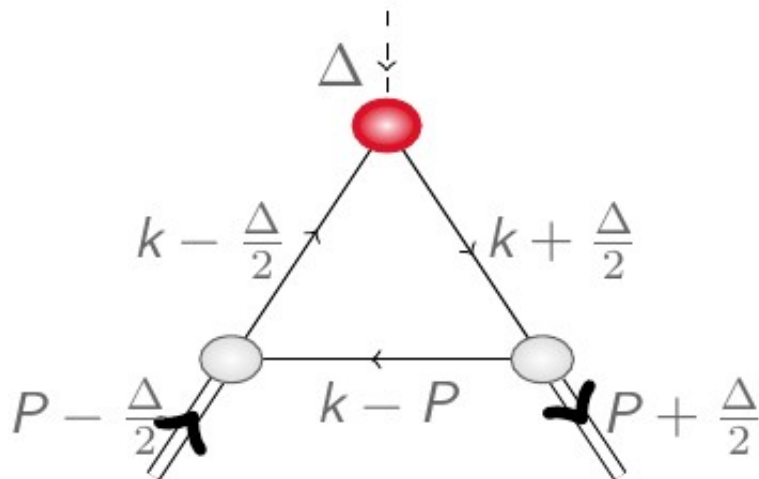
- Compute **Mellin moments** of the pion GPD H .

Antecedents:

GPDs in the Schwinger-Dyson and Bethe-Salpeter approach



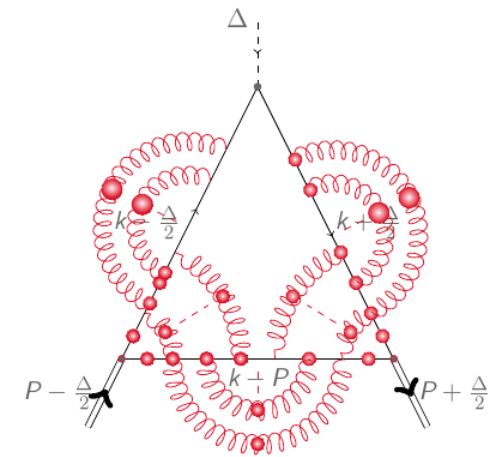
$$\langle x^m \rangle^q = \frac{1}{2(P^+)^{n+1}} \left\langle \pi, P + \frac{\Delta}{2} \left| \bar{q}(0) \gamma^+ (i \overleftrightarrow{D}^+)^m q(0) \right| \pi, P - \frac{\Delta}{2} \right\rangle$$



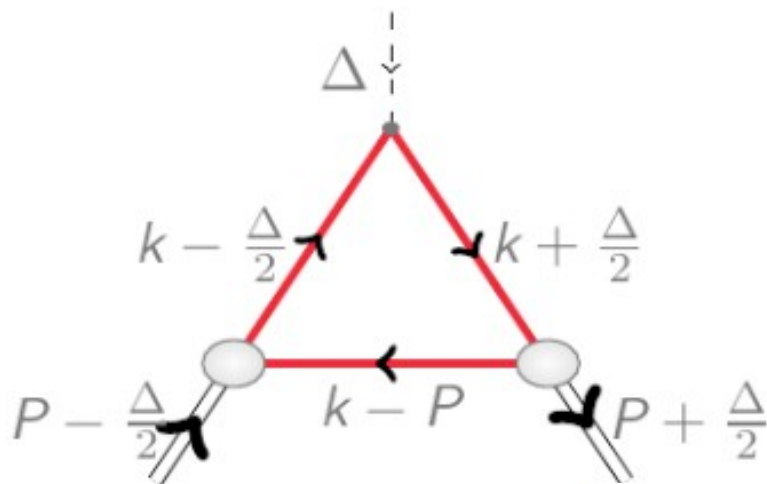
- Compute **Mellin moments** of the pion GPD H .
- Triangle diagram approx.

Antecedents:

GPDs in the Schwinger-Dyson and Bethe-Salpeter approach



$$\langle x^m \rangle^q = \frac{1}{2(P^+)^{n+1}} \left\langle \pi, P + \frac{\Delta}{2} \left| \bar{q}(0) \gamma^+ (i \overleftrightarrow{D}^+)^m q(0) \right| \pi, P - \frac{\Delta}{2} \right\rangle$$



- Compute **Mellin moments** of the pion GPD H .
- Triangle diagram approx.
- Resum **infinitely many** contributions.

Dyson - Schwinger equation

$$\text{---} \circ \text{---}^{-1} = \text{---}^{-1} + \text{---} \circ \text{---} \text{---} \circ \text{---}^{-1}$$

Antecedents:

GPD asymptotic algebraic model:

- Expressions for vertices and propagators:

$$S(p) = [-i\gamma \cdot p + M] \Delta_M(p^2)$$

$$\Delta_M(s) = \frac{1}{s + M^2}$$

$$\Gamma_\pi(k, p) = i\gamma_5 \frac{M}{f_\pi} M^{2\nu} \int_{-1}^{+1} dz \rho_\nu(z) [\Delta_M(k_{+z}^2)]^\nu$$

$$\rho_\nu(z) = R_\nu (1 - z^2)^\nu$$

with R_ν a normalization factor and $k_{+z} = k - p(1 - z)/2$.

Chang et al., Phys. Rev. Lett. **110** 132001 (2013)

- Only two parameters:

- Dimensionful
- Dimensionless asympt.

See Cedric's talk!

Antecedents:

GPD asymptotic algebraic model:

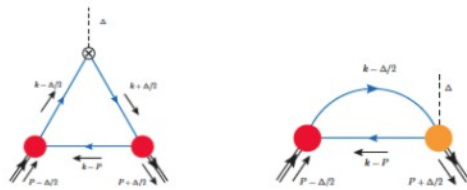
- Analytic expression in the DGLAP region.

$$H_{x \geq \xi}^u(x, \xi, 0) = \frac{48}{5} \left\{ \frac{3 \left(-2(x-1)^4 (2x^2 - 5\xi^2 + 3) \log(1-x) \right)}{20(\xi^2 - 1)^3} \right. \\ + \frac{3 \left(+4\xi \left(15x^2(x+3) + (19x+29)\xi^4 + 5(x(x(x+11)+21)+3)\xi^2 \right) \tanh^{-1} \left(\frac{x-1}{x-\xi^2} \right) \right)}{20(\xi^2 - 1)^3} \\ + \frac{3 \left(x^3(x(2(x-4)x+15)-30) - 15(2x(x+5)+5)\xi^4 \right) \log(x^2 - \xi^2)}{20(\xi^2 - 1)^3} \\ + \frac{3 \left(-5x(x(x(x+2)+36) + 18)\xi^2 - 15\xi^6 \right) \log(x^2 - \xi^2)}{20(\xi^2 - 1)^3} \\ + \frac{3 \left(2(x-1) \left((23x+58)\xi^4 + (x(x(x+67)+112)+6)\xi^2 + x(x((5-2x)x+15) + \dots \right) \right)}{20(\xi^2 - 1)^3} \\ \left. + \frac{3 \left(-5\xi^4 + 10x(3x(x+5)+11)\xi^2 \right) \log(1-\xi^2)}{20(\xi^2 - 1)^3} \right\}$$

Antecedents:

GPD asymptotic algebraic model (completion):

The full model:



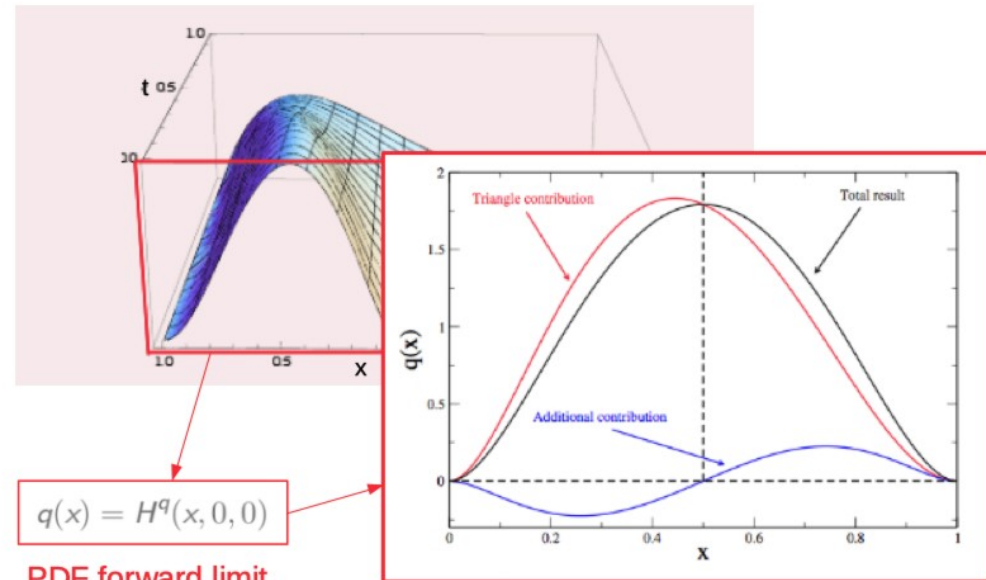
$$2(P \cdot n)^{m+1} \langle x^m \rangle^u = \text{tr}_{CFD} \int \frac{d^4 k}{(2\pi)^4} (k \cdot n)^m \tau_+ i\bar{\Gamma}_\pi \left(\eta(k-P) + (1-\eta) \left(k - \frac{\Delta}{2} \right), P - \frac{\Delta}{2} \right) \\ S(k - \frac{\Delta}{2}) i\gamma \cdot n S(k + \frac{\Delta}{2}) \\ \tau_- i\bar{\Gamma}_\pi \left((1-\eta) \left(k + \frac{\Delta}{2} \right) + \eta(k-P), P + \frac{\Delta}{2} \right) S(k-P),$$

$$2(P \cdot n)^{m+1} \langle x^m \rangle^u = \text{tr}_{CFD} \int \frac{d^4 k}{(2\pi)^4} (k \cdot n)^m \tau_+ i\bar{\Gamma}_\pi \left(\eta(k-P) + (1-\eta) \left(k - \frac{\Delta}{2} \right), P - \frac{\Delta}{2} \right) \\ S(k - \frac{\Delta}{2}) \tau_- \frac{\partial}{\partial k} \bar{\Gamma}_\pi \left((1-\eta) \left(k + \frac{\Delta}{2} \right) + \eta(k-P), P + \frac{\Delta}{2} \right) S(k-P)$$

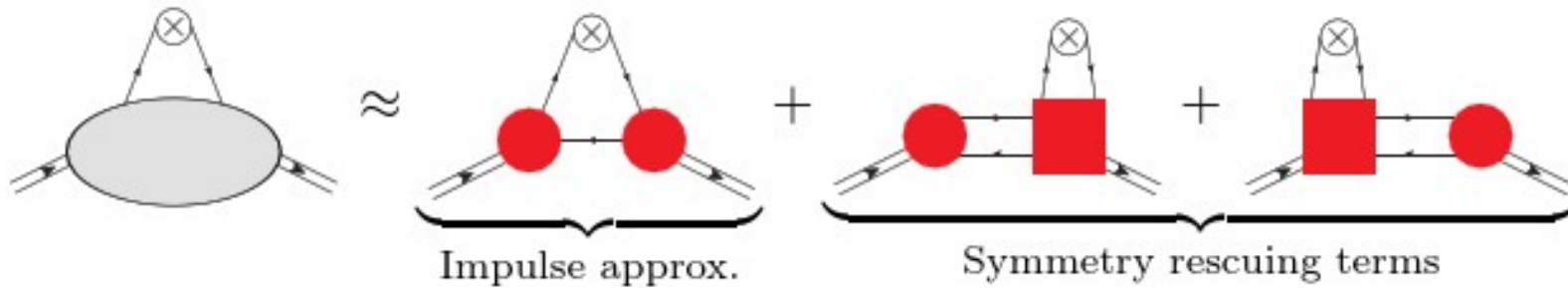
C. Mezrag et al., PLB741(2015)190; ArXiv:1406.7425[hep-ph]

Antecedents:

GPD asymptotic algebraic model (completion):



GPD asymptotic algebraic model:



L.Chang et al., Phys.Lett. B737 (2014) 23-29

Asymptotic algebraic model:

region.

$$\frac{2(1+3)\xi^2 \tanh^{-1}\left(\frac{x-1}{x-\xi^2}\right)}{\xi^2}$$

See Cédric's talk!

$$q(x) = H^q(x, 0, 0)$$

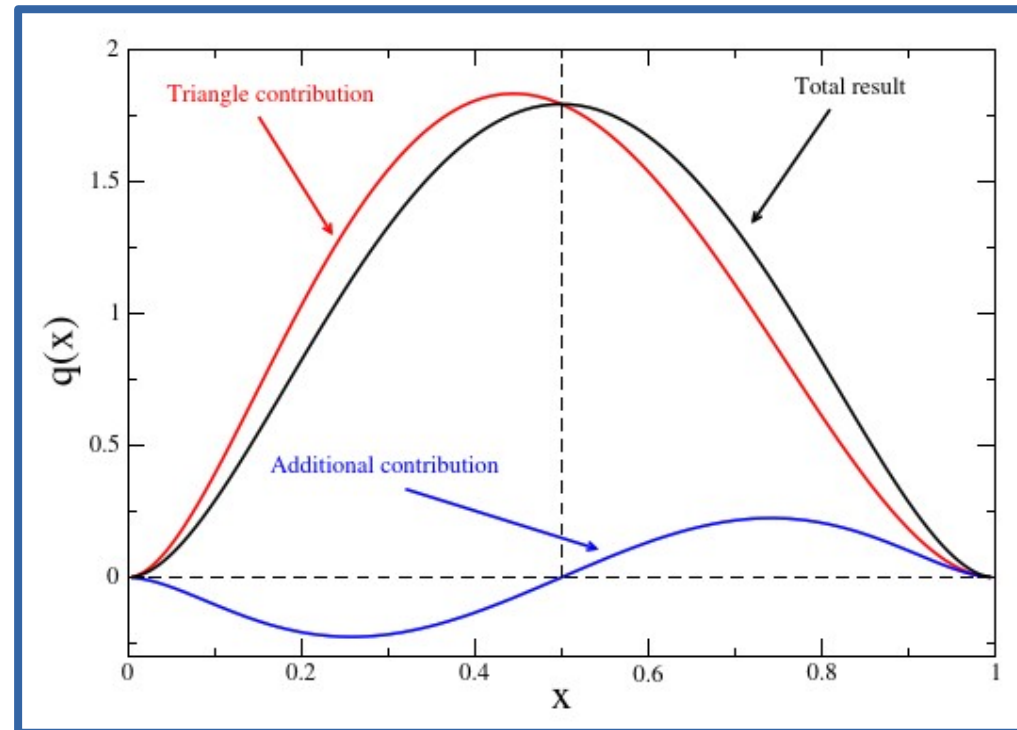
$$2(P \cdot n)^{m+1} \langle x^m \rangle$$

...

$$\tau_- i \bar{\Gamma}_\pi \left((1 - \dots) \right)$$

$$2(P \cdot n)^{m+1} \langle x^m \rangle = \text{tr}_{CFD} \int \frac{d^4 k}{(2\pi)^4} (k \cdot n)^m \tau_+ i \bar{\Gamma}_\pi \left(\eta(k-P) + (1 - \dots) \right) S(k - \frac{\Delta}{2}) \tau_- \frac{\partial}{\partial k} \bar{\Gamma}_\pi \left((1 - \eta) \left(k + \frac{\Delta}{2} \right) + \eta(k-P), P + \frac{\Delta}{2} \right) S(k-P)$$

C. Mezrag et al., PLB741(2015)190; ArXiv:1406.7425[hep-ph]



GPD overlap approach:

The overlap quark GPD for a meson in the DGLAP kinematic region reads

$$H^q(x, \xi, t) = \sum_{N, \beta} \sqrt{1 - \xi}^{2-N} \sqrt{1 + \xi}^{2-N} \sum_a \delta_{a, q} \int [d\bar{x}]_N [d^2\bar{\mathbf{k}}_\perp]_N \delta(x - \bar{x}_a) \\ \times \Psi_{N, \beta}^* \left(\hat{x}'_1, \hat{\mathbf{k}}'_{\perp 1}, \dots, \hat{x}'_a, \hat{\mathbf{k}}'_{\perp a}, \dots \right) \Psi_{N, \beta} \left(\bar{x}_1, \bar{\mathbf{k}}_{\perp 1}, \dots, \bar{x}_a, \bar{\mathbf{k}}_{\perp a}, \dots \right),$$

$$[dx]_N = \prod_{i=1}^N dx_i \delta \left(1 - \sum_{i=1}^N x_i \right),$$

$$[d^2\mathbf{k}_\perp]_N = \frac{1}{(16\pi^3)^{N-1}} \prod_{i=1}^N d^2\mathbf{k}_{\perp i} \delta^2 \left(\sum_{i=1}^N \mathbf{k}_{\perp i} - \mathbf{P}_\perp \right).$$

GPD overlap approach:

The overlap quark GPD for a meson in the DGLAP kinematic region reads

$$H^q(x, \xi, t) = \sum_{N, \beta} \sqrt{1 - \xi}^{2-N} \sqrt{1 + \xi}^{2-N} \sum_a \delta_{a,q} \int [d\bar{x}]_N [d^2\bar{\mathbf{k}}_\perp]_N \delta(x - \bar{x}_a) \\ \times \Psi_{N, \beta}^* \left(\hat{x}'_1, \hat{\mathbf{k}}'_{\perp 1}, \dots, \hat{x}'_a, \hat{\mathbf{k}}'_{\perp a}, \dots \right) \Psi_{N, \beta} \left(\bar{x}_1, \bar{\mathbf{k}}_{\perp 1}, \dots, \bar{x}_a, \bar{\mathbf{k}}_{\perp a}, \dots \right),$$

$$[dx]_N = \prod_{i=1}^N dx_i \delta \left(1 - \sum_{i=1}^N x_i \right),$$

in terms of the meson LFWF

$$[d^2\mathbf{k}_\perp]_N = \frac{1}{(16\pi^3)^{N-1}} \prod_{i=1}^N d^2\mathbf{k}_{\perp i} \delta^2 \left(\sum_{i=1}^N \mathbf{k}_{\perp i} - \mathbf{P}_\perp \right).$$

$$|H; P, \lambda\rangle = \sum_{N, \beta} \int [dx]_N [d^2\mathbf{k}_\perp]_N \Psi_{N, \beta}^\lambda(x_1, \mathbf{k}_{\perp 1}, \dots, x_N, \mathbf{k}_{\perp N}) |N, \beta; k_1, \dots, k_N\rangle$$

which are the components in an expansion of the meson on a Fock basis, after light-front quantization.

GPD overlap approach:

The overlap **valence-quark** GPD for a meson in the DGLAP kinematic region reads

$$H^q(x, \xi, t) = \int \frac{d^2\mathbf{k}_\perp}{16\pi^3} \Psi_{u\bar{f}}^* \left(\frac{x-\xi}{1-\xi}, \mathbf{k}_\perp + \frac{1-x}{1-\xi} \frac{\Delta_\perp}{2} \right) \Psi_{u\bar{f}} \left(\frac{x+\xi}{1+\xi}, \mathbf{k}_\perp - \frac{1-x}{1+\xi} \frac{\Delta_\perp}{2} \right)$$

GPD overlap approach:

The overlap **valence-quark** GPD for a meson in the DGLAP kinematic region reads

$$H^q(x, \xi, t) = \int \frac{d^2\mathbf{k}_\perp}{16\pi^3} \Psi_{u\bar{f}}^* \left(\frac{x-\xi}{1-\xi}, \mathbf{k}_\perp + \frac{1-x}{1-\xi} \frac{\Delta_\perp}{2} \right) \Psi_{u\bar{f}} \left(\frac{x+\xi}{1+\xi}, \mathbf{k}_\perp - \frac{1-x}{1+\xi} \frac{\Delta_\perp}{2} \right)$$

$$2P^+ \psi_{\uparrow\downarrow}(k^+, \mathbf{k}_\perp) = \int \frac{dk^-}{2\pi} \text{Tr}[\gamma^+ \gamma_5 \chi(k, P)]$$

GPD overlap approach:

The overlap **valence-quark** GPD for a meson in the DGLAP kinematic region reads

$$H^q(x, \xi, t) = \int \frac{d^2\mathbf{k}_\perp}{16\pi^3} \Psi_{u\bar{f}}^* \left(\frac{x-\xi}{1-\xi}, \mathbf{k}_\perp + \frac{1-x}{1-\xi} \frac{\Delta_\perp}{2} \right) \Psi_{u\bar{f}} \left(\frac{x+\xi}{1+\xi}, \mathbf{k}_\perp - \frac{1-x}{1+\xi} \frac{\Delta_\perp}{2} \right)$$

$$\Gamma_\pi(q, P) = iN\gamma_5 \int_0^\infty d\omega \int_{-1}^1 dz \frac{\rho(\omega, z)M^2}{\left(q - \frac{1-z}{2}P\right)^2 + M^2 + \omega}$$

$$\chi(q, P) = S(q) \Gamma_\pi(q, P) S(q - P)$$

$$2P^+ \psi_{\uparrow\downarrow}(k^+, \mathbf{k}_\perp) = \int \frac{dk^-}{2\pi} \text{Tr} [\gamma^+ \gamma_5 \chi(k, P)]$$

Bethe-Salpeter amplitudes and quark propagators can be obtained from applying continuum functional methods (DSE, BSE)

GPD overlap approach:

The overlap **valence-quark** GPD for a meson in the DGLAP kinematic region reads

$$H^q(x, \xi, t) = \int \frac{d^2\mathbf{k}_\perp}{16\pi^3} \Psi_{u\bar{f}}^* \left(\frac{x-\xi}{1-\xi}, \mathbf{k}_\perp + \frac{1-x}{1-\xi} \frac{\Delta_\perp}{2} \right) \Psi_{u\bar{f}} \left(\frac{x+\xi}{1+\xi}, \mathbf{k}_\perp - \frac{1-x}{1+\xi} \frac{\Delta_\perp}{2} \right)$$

$$S(q) = [-i\gamma \cdot q + M]/[q^2 + M^2] \quad \text{Nakanishi weight}$$

$$\Gamma_\pi(q, P) = iN\gamma_5 \int_0^\infty d\omega \int_{-1}^1 dz \frac{\rho(\omega, z) M^2}{(q - \frac{1-z}{2}P)^2 + M^2 + \omega}$$

$$\chi(q, P) = S(q) \Gamma_\pi(q, P) S(q-P)$$

$$2P^+ \psi_{\uparrow\downarrow}(k^+, \mathbf{k}_\perp) = \int \frac{dk^-}{2\pi} \text{Tr}[\gamma^+ \gamma_5 \chi(k, P)]$$

Asymptotic case: $\rho(w, z) = \delta(w)(1 - z^2)$

Bethe-Salpeter amplitudes and quark propagators can be obtained from applying continuum functional methods (DSE, BSE) or can be modeled as previously indicated.

GPD overlap approach:

The overlap **valence-quark** GPD for a meson in the DGLAP kinematic region reads

$$H^q(x, \xi, t) = 30 \frac{(1-x)^2(x^2 - \xi^2)}{(1-\xi^2)^2} \frac{1}{(1+z)^2} \left(\frac{3}{4} + \frac{1}{4} \frac{1-2z}{1+z} \frac{\operatorname{arctanh} \sqrt{\frac{z}{1+z}}}{\sqrt{\frac{z}{1+z}}} \right)$$

$$z = \frac{t}{4M^2} \frac{(1-x)^2}{1-\xi^2}$$

Encoding the correlation of kinematical variables

$$S(q) = [-i\gamma \cdot q + M]/[q^2 + M^2] \quad \text{Nakanishi weight}$$

$$\Gamma_\pi(q, P) = iN\gamma_5 \int_0^\infty d\omega \int_{-1}^1 dz \frac{\rho(\omega, z) M^2}{(q - \frac{1-z}{2}P)^2 + M^2 + \omega}$$

$$\chi(q, P) = S(q) \Gamma_\pi(q, P) S(q - P)$$

Asymptotic case: $\rho(w, z) = \delta(w)(1 - z^2)$

Bethe-Salpeter amplitudes and quark propagators can be obtained from applying continuum functional methods (DSE, BSE) or can be modeled as previously indicated.

GPD overlap approach:

The overlap **valence-quark** GPD for a meson in the DGLAP kinematic region reads

$$H^q(x, \xi, t) = 30 \frac{(1-x)^2(x^2 - \xi^2)}{(1-\xi^2)^2} \frac{1}{(1+z)^2} \left(\frac{3}{4} + \frac{1}{4} \frac{1-2z}{1+z} \frac{\operatorname{arctanh} \sqrt{\frac{z}{1+z}}}{\sqrt{\frac{z}{1+z}}} \right) = 30 x^2(1-x)^2$$

$$z = \frac{t}{4M^2} \frac{(1-x)^2}{1-\xi^2}$$

Encoding the correlation of kinematical variables

$$S(q) = [-i\gamma \cdot q + M]/[q^2 + M^2]$$

Nakanishi weight

Forward limit:

$$\xi = 0, t = 0$$

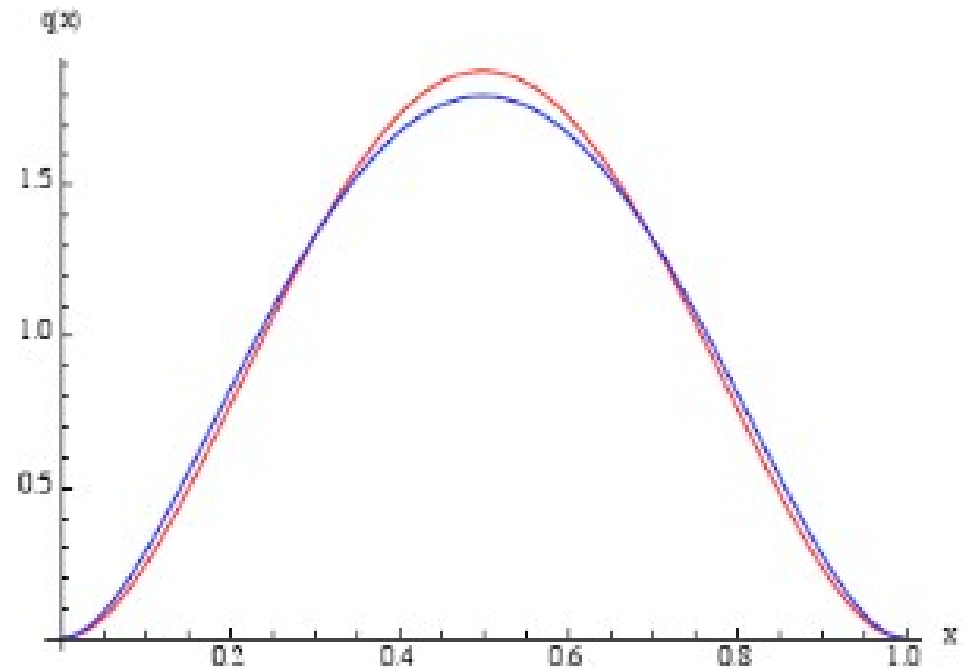
$$\Gamma_\pi(q, P) = iN\gamma_5 \int_0^\infty d\omega \int_{-1}^1 dz \frac{\rho(\omega, z) M^2}{(q - \frac{1-z}{2}P)^2 + M^2 + \omega}$$

$$\chi(q, P) = S(q) \Gamma_\pi(q, P) S(q - P)$$

— Overlap — Triangle diagram

Asymptotic case: $\rho(w, z) = \delta(w)(1 - z^2)$

Bethe-Salpeter amplitudes and quark propagators can be obtained from applying continuum functional methods (DSE, BSE) or can be modeled as previously indicated.



GPD overlap approach:

The overlap **valence-quark** GPD for a meson in the DGLAP kinematic region reads

$$H^q(x, \xi, t) = 30 \frac{(1-x)^2(x^2 - \xi^2)}{(1-\xi^2)^2} \frac{1}{(1+z)^2} \left(\frac{3}{4} + \frac{1}{4} \frac{1-2z}{1+z} \frac{\operatorname{arctanh} \sqrt{\frac{z}{1+z}}}{\sqrt{\frac{z}{1+z}}} \right) = 30 x^2(1-x)^2$$

$$z = \frac{t}{4M^2} \frac{(1-x)^2}{1-\xi^2}$$

Encoding the correlation of kinematical variables

$$S(q) = [-i\gamma \cdot q + M]/[q^2 + M^2]$$

Nakanishi weight

Forward limit:

$$\xi = 0, t = 0$$

$$\Gamma_\pi(q, P) = iN\gamma_5 \int_0^\infty d\omega \int_{-1}^1 dz \frac{\rho(\omega, z) M^2}{(q - \frac{1-z}{2}P)^2 + M^2 + \omega}$$

$$\chi(q, P) = S(q) \Gamma_\pi(q, P) S(q - P)$$

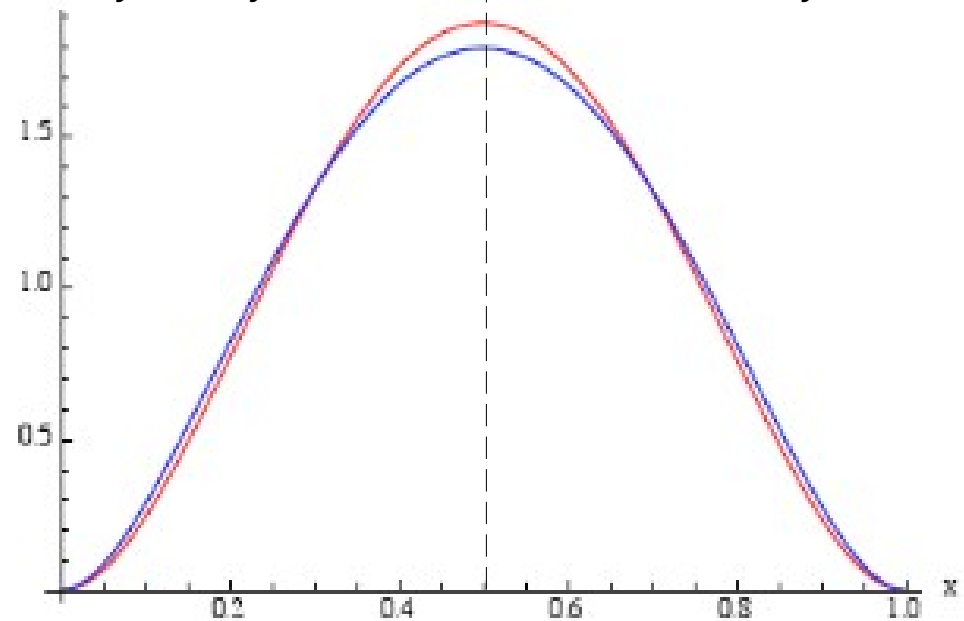
Asymptotic case: $\rho(w, z) = \delta(w)(1 - z^2)$

Bethe-Salpeter amplitudes and quark propagators can be obtained from applying continuum functional methods (DSE, BSE) or can be modeled as previously indicated.

Results from the overlap and diagrammatic approaches compare very well (tested at the level of the PDF).

— Overlap — Triangle diagram

q^2 symmetry under: $x \leftrightarrow 1 - x$ is a key feature!



Integral representation of LFWFs:

See tomorrow Khépani's talk!

- The pseudoscalar LFWF can be written:

$$f_K \psi_K^{\uparrow\downarrow}(x, k_{\perp}^2) = \text{tr}_{CD} \int_{dk_{\parallel}} \delta(n \cdot k - x n \cdot P_K) \gamma_5 \gamma \cdot n \chi_K^{(2)}(k_{\perp}^K; P_K).$$

- The moments of the distribution are given by:

$$\langle x^m \rangle_{\psi_K^{\uparrow\downarrow}} = \int_0^1 dx x^m \psi_K^{\uparrow\downarrow}(x, k_{\perp}^2) = \frac{1}{f_K n \cdot P} \int_{dk_{\parallel}} \left[\frac{n \cdot k}{n \cdot P} \right]^m \gamma_5 \gamma \cdot n \chi_K^{(2)}(k_{\perp}^K; P_K)$$

$$\int_0^1 d\alpha \alpha^m \left[\frac{12}{f_K} \mathcal{Y}_K(\alpha; \sigma^2) \right], \quad \mathcal{Y}_K(\alpha; \sigma^2) = [M_u(1 - \alpha) + M_s \alpha] \mathcal{X}(\alpha; \sigma_{\perp}^2).$$

Uniqueness of Mellin moments



$$\psi_K^{\uparrow\downarrow}(x, k_{\perp}^2) = \frac{12}{f_K} \mathcal{Y}_K(x; \sigma_{\perp}^2)$$

$$\chi_K(\alpha; \sigma^3) = \left[\int_{-1}^{1-2\alpha} d\omega \int_{1+\frac{2\alpha}{\omega-1}}^1 dv + \int_{1-2\alpha}^1 d\omega \int_{\frac{\omega-1+2\alpha}{\omega+1}}^1 dv \right] \frac{\rho_K(\omega) \Lambda_K^2}{n_K \sigma^3}.$$



$$\Rightarrow \psi_K^{\uparrow\downarrow}(x, k_{\perp}^2) \sim \int d\omega \cdots \rho_K(\omega) \cdots$$

The Nakanishi weight $\rho_K(z)$ can be modeled...

...Or taken with BSE solutions as an input!

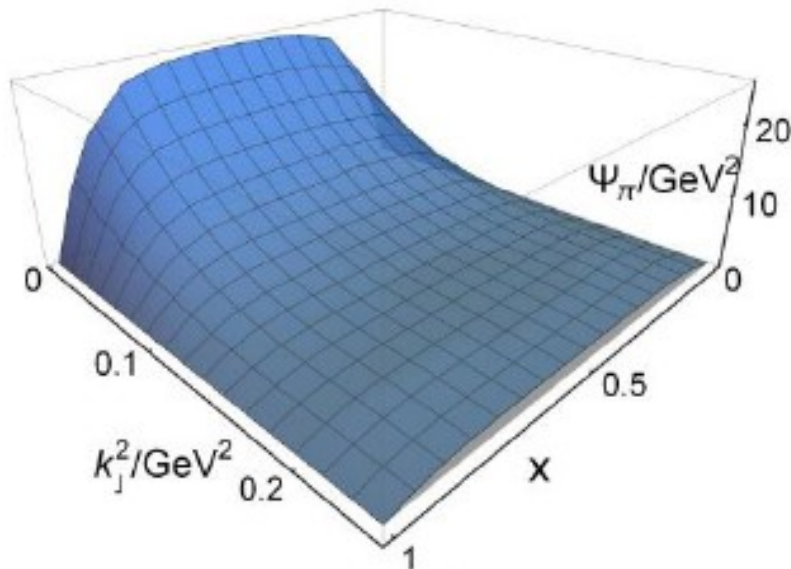
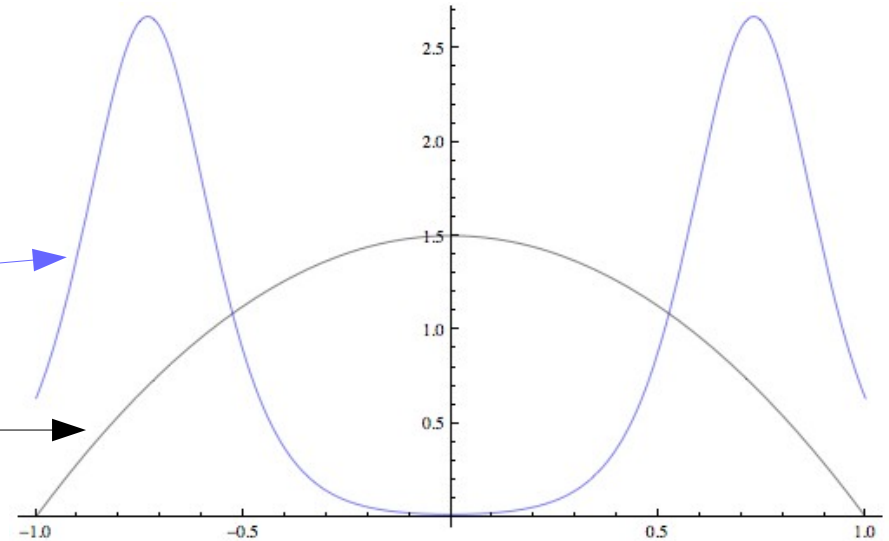
Integral representation of LFWFs: pion case

Nakanishi weight parametrization:

$$\rho(z) = \frac{1}{2b_0} \left[\operatorname{sech}^2 \left(\frac{z - z_0}{2b_0} \right) + \operatorname{sech}^2 \left(\frac{z + z_0}{2b_0} \right) \right]$$

Phenomenological model: $b_0^\pi = 0.1, z_0^\pi = 0.73$;

Asymptotic case: $\rho(z) = (1 - z^2)$



Integral representation of LFWFs:

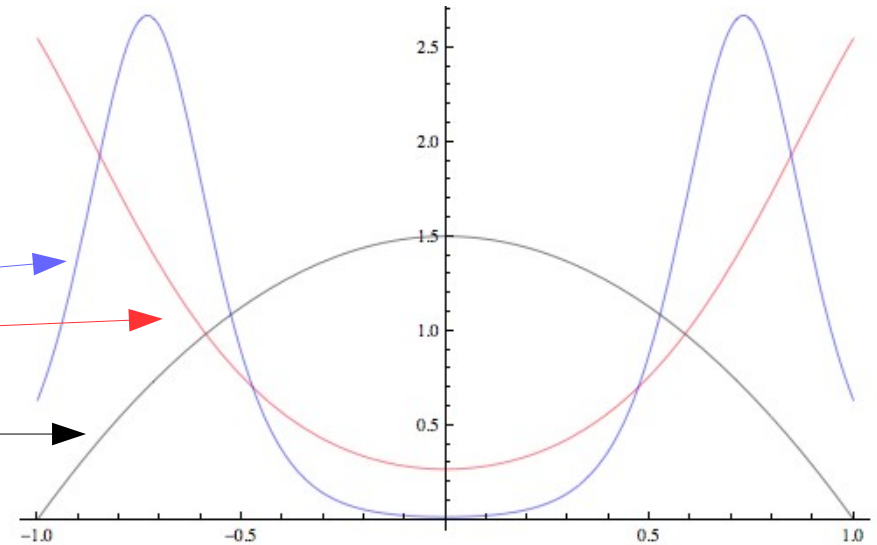
Nakanishi weight parametrization:

$$\rho(z) = \frac{1}{2b_0} \left[\operatorname{sech}^2 \left(\frac{z - z_0}{2b_0} \right) + \operatorname{sech}^2 \left(\frac{z + z_0}{2b_0} \right) \right]$$

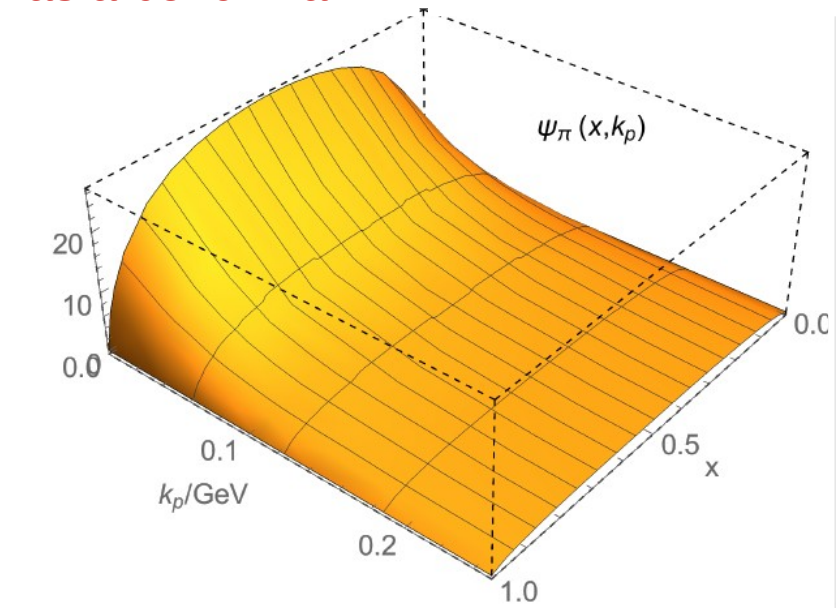
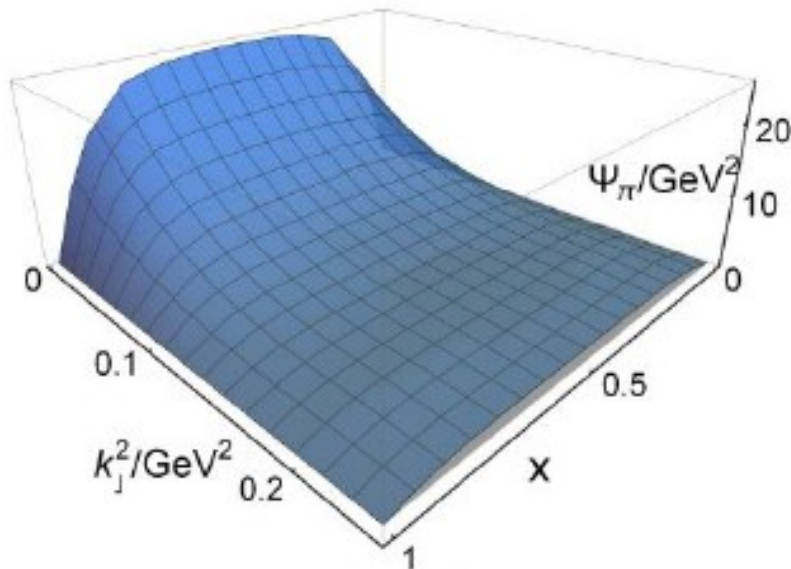
Phenomenological model: $b_0^\pi = 0.1, z_0^\pi = 0.73$;

Realistic case: $b_0^\pi = 0.275, z_0^\pi = 1.23$;

Asymptotic case: $\rho(z) = (1 - z^2)$



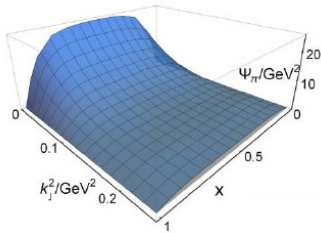
See Khépani's talk: PDF as a benchmark!



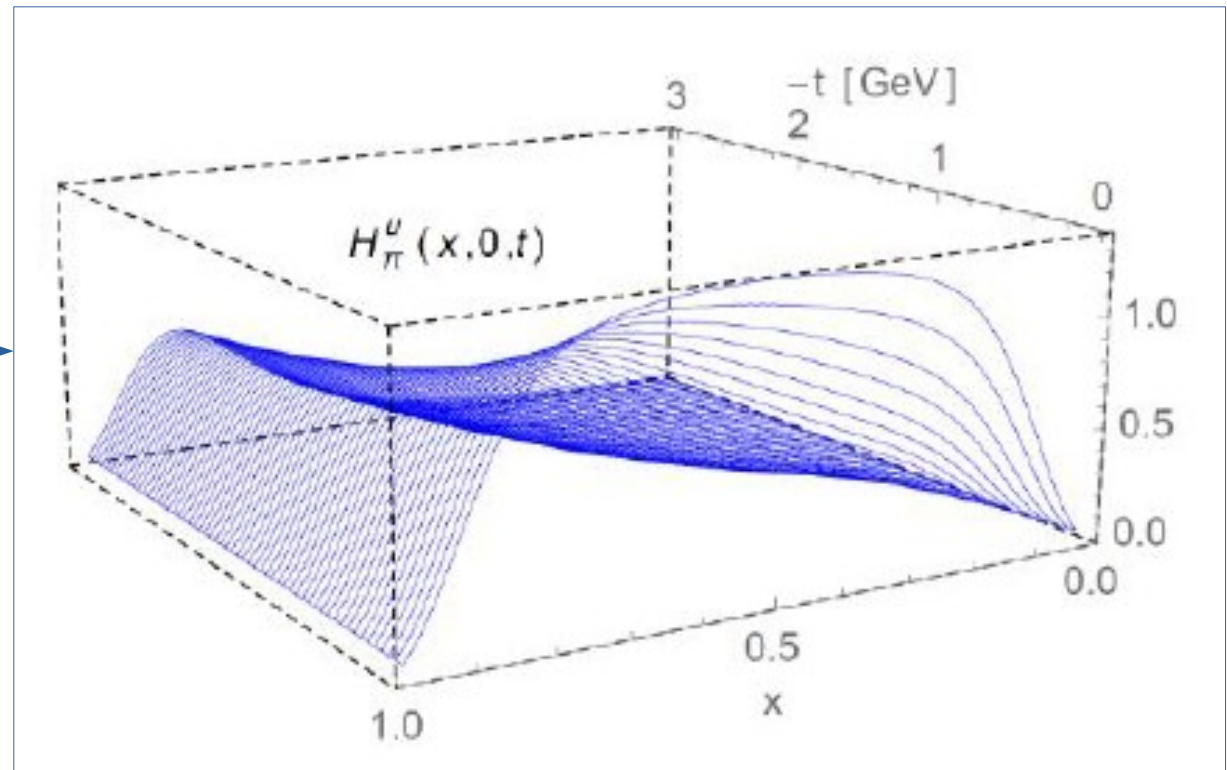
GPD overlap approach: pion case

The overlap **valence-quark** GPD for a meson in the DGLAP kinematic region reads

$$H^q(x, \xi, t) = \int \frac{d^2 \mathbf{k}_\perp}{16 \pi^3} \Psi_{u\bar{f}}^* \left(\frac{x - \xi}{1 - \xi}, \mathbf{k}_\perp + \frac{1 - x}{1 - \xi} \frac{\Delta_\perp}{2} \right) \Psi_{u\bar{f}} \left(\frac{x + \xi}{1 + \xi}, \mathbf{k}_\perp - \frac{1 - x}{1 + \xi} \frac{\Delta_\perp}{2} \right)$$



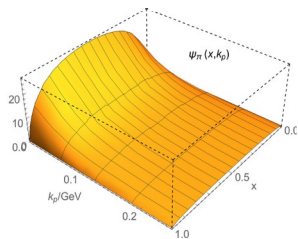
Phenomenological model



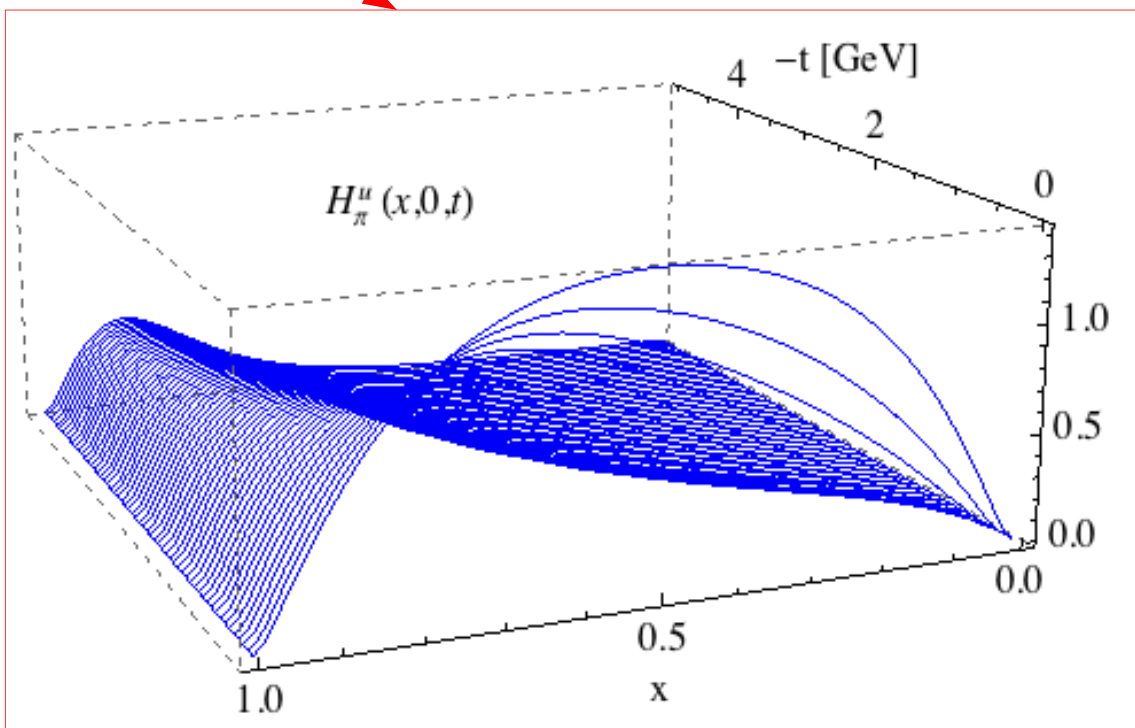
GPD overlap approach: pion case

The overlap **valence-quark** GPD for a meson in the DGLAP kinematic region reads

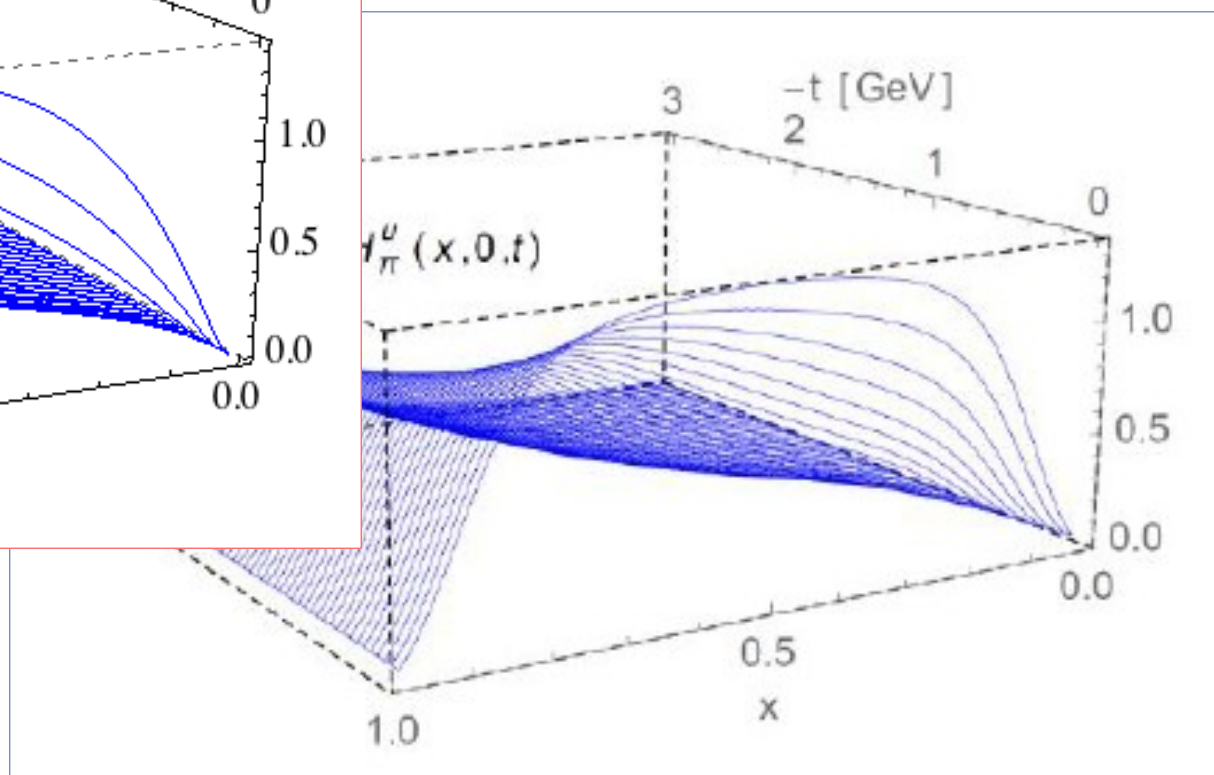
$$H^q(x, \xi, t) = \int \frac{d^2 \mathbf{k}_\perp}{16 \pi^3} \Psi_{u\bar{f}}^* \left(\frac{x - \xi}{1 - \xi}, \mathbf{k}_\perp + \frac{1 - x}{1 - \xi} \frac{\Delta_\perp}{2} \right) \Psi_{u\bar{f}} \left(\frac{x + \xi}{1 + \xi}, \mathbf{k}_\perp - \frac{1 - x}{1 + \xi} \frac{\Delta_\perp}{2} \right)$$



Phenomenological model



Realistic case

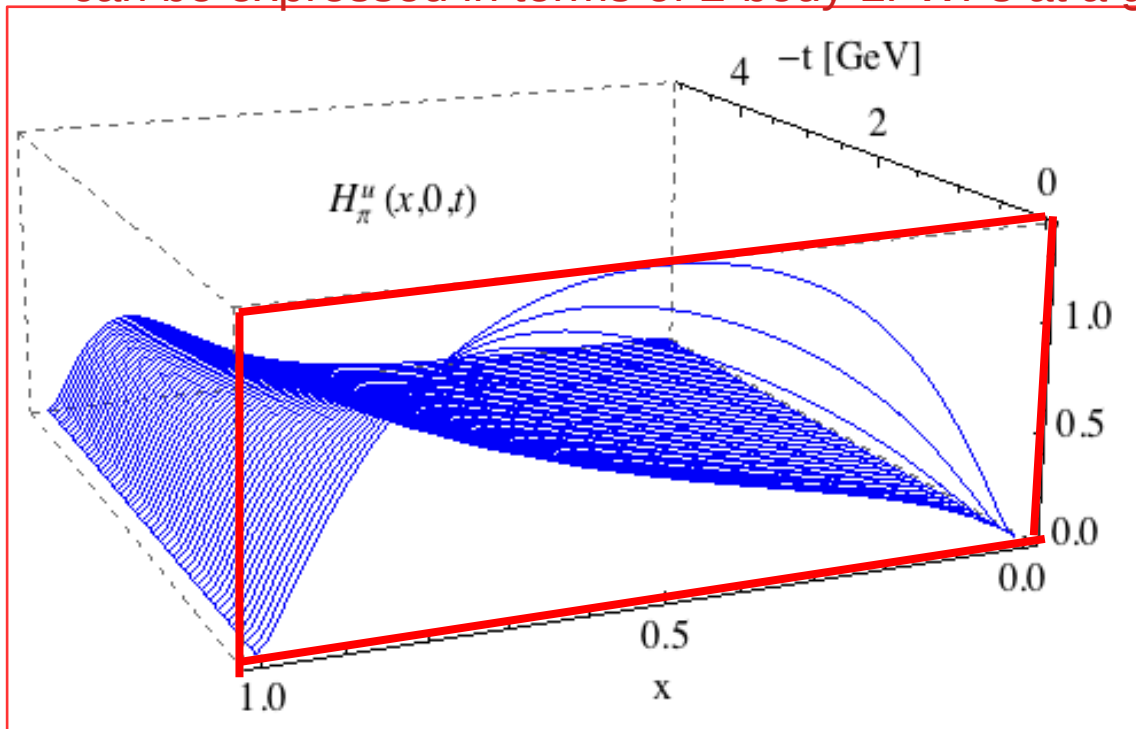


GPD overlap approach: pion case

The overlap **valence-quark** GPD for a meson in the DGLAP kinematic region reads

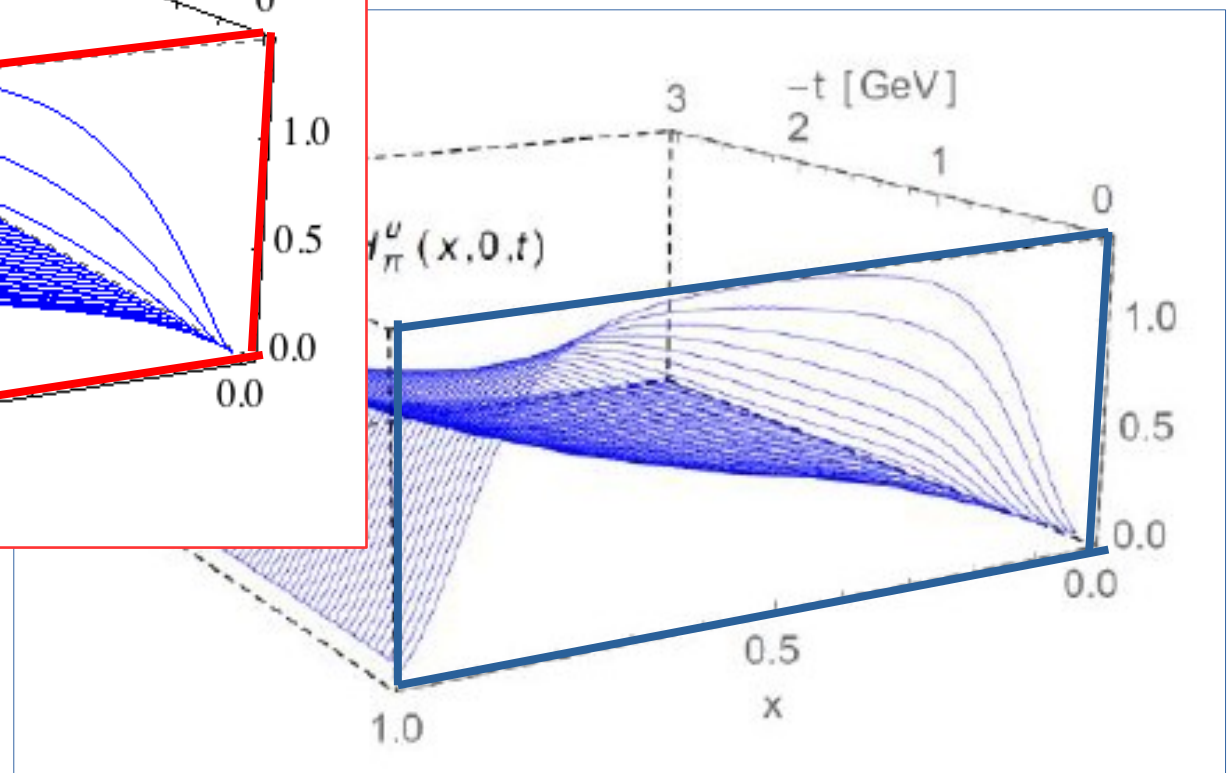
$$H^q(x, \xi, t) = \int \frac{d^2 \mathbf{k}_\perp}{16 \pi^3} \Psi_{u\bar{f}}^*(x, \mathbf{k}_\perp) \Psi_{u\bar{f}}(x, \mathbf{k}_\perp) = q^\pi(x; \zeta_H)$$

Focus on the forward limit: the PDF that, in the overlap representation at low Fock space, can be expressed in terms of 2-body LFWFs at a given hadronic scale



Realistic case

Phenomenological model



GPD overlap approach: pion case

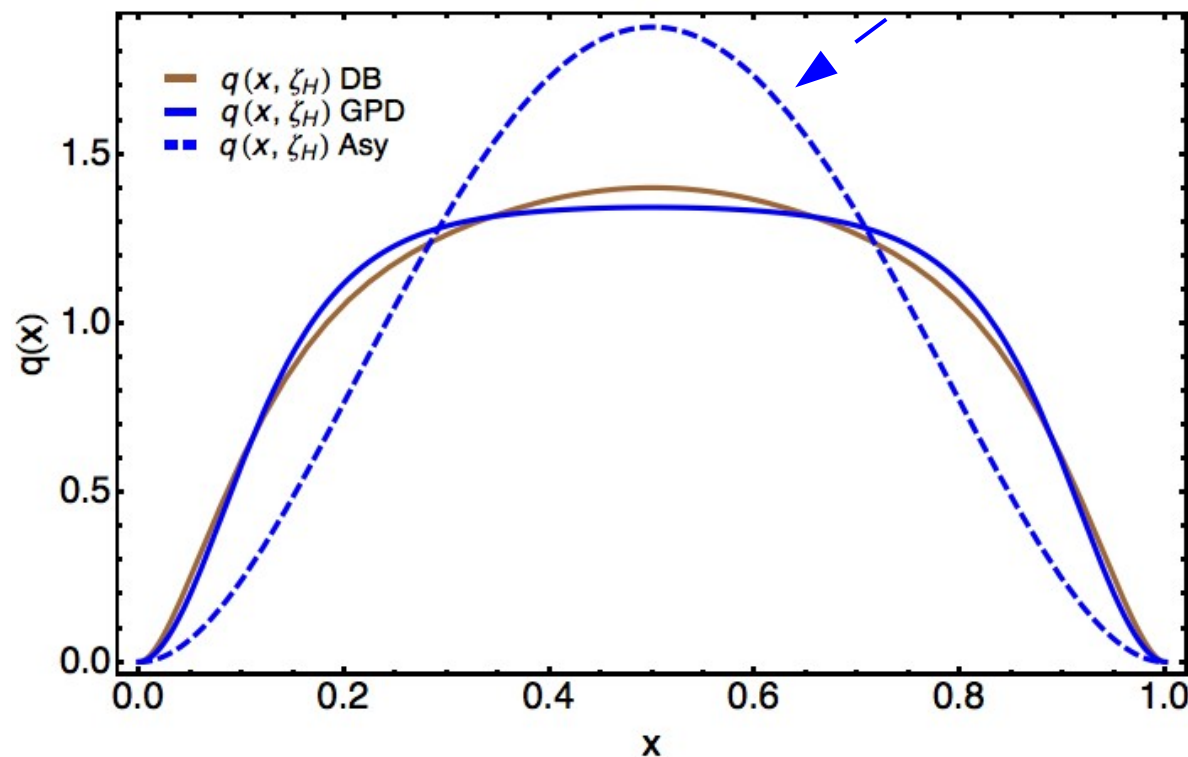
The overlap **valence-quark** GPD for a meson in the DGLAP kinematic region reads

$$H^q(x, \xi, t) = \int \frac{d^2\mathbf{k}_\perp}{16\pi^3} \Psi_{u\bar{f}}^*(x, \mathbf{k}_\perp) \Psi_{u\bar{f}}(x, \mathbf{k}_\perp) = q^\pi(x; \zeta_H)$$

Focus on the forward limit: the PDF that, in the overlap representation at low Fock space, can be expressed in terms of 2-body LFWFs at a given hadronic scale

$$q^\pi(x; \zeta_H) = 30x^2(1-x)^2$$

LFWF leading to asymptotic PDA



GPD overlap approach: pion case

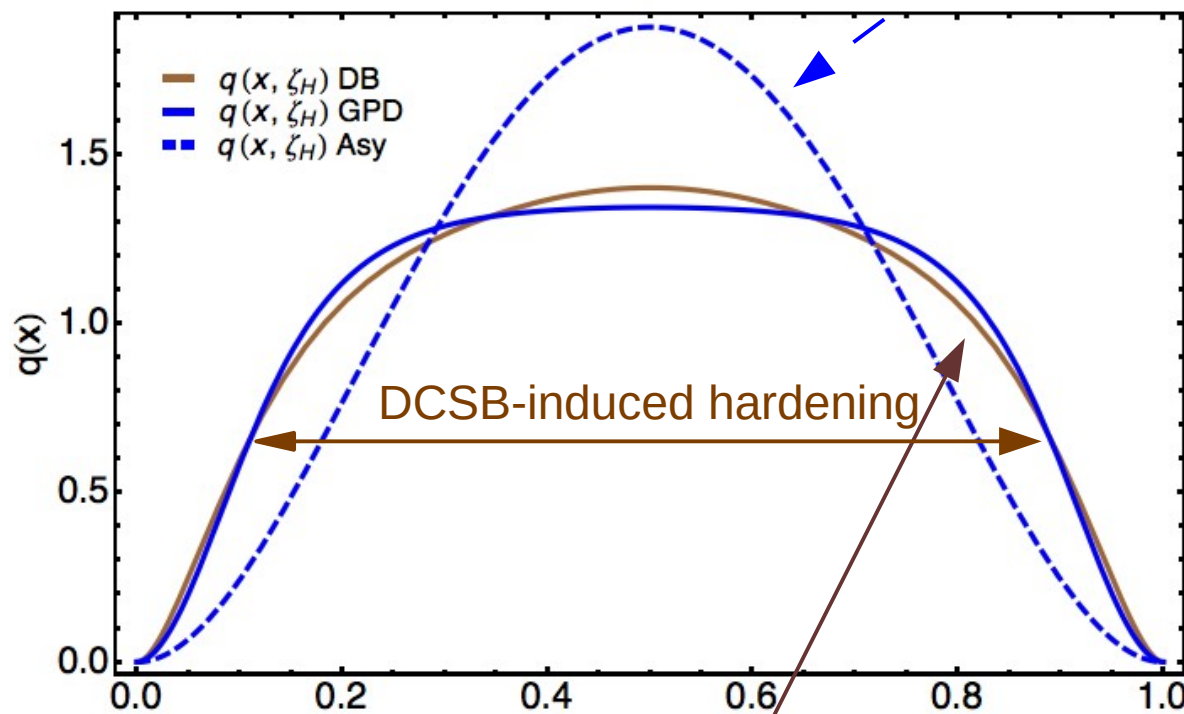
The overlap **valence-quark** GPD for a meson in the DGLAP kinematic region reads

$$H^q(x, \xi, t) = \int \frac{d^2\mathbf{k}_\perp}{16\pi^3} \Psi_{u\bar{f}}^*(x, \mathbf{k}_\perp) \Psi_{u\bar{f}}(x, \mathbf{k}_\perp) = q^\pi(x; \zeta_H)$$

Focus on the forward limit: the PDF that, in the overlap representation at low Fock space, can be expressed in terms of 2-body LFWFs at a given hadronic scale

$$q^\pi(x; \zeta_H) = 30x^2(1-x)^2$$

LFWF leading to asymptotic PDA



Direct computation of Mellin moments:

$$\langle x^m \rangle_{\zeta_H}^\pi = \int_0^1 dx x^m q^\pi(x; \zeta_H)$$

$$= \frac{N_c}{n \cdot P} \text{tr} \int_{dk} \left[\frac{n \cdot k_\eta}{n \cdot P} \right]^m \Gamma_\pi(k_{\bar{\eta}}, P) S(k_{\bar{\eta}}) n \cdot \partial_{k_\eta} [\Gamma_\pi(k_\eta, -P) S(k_\eta)]$$

M. Ding et al., PRD01(2020)054014

$$q^\pi(x; \zeta_H) = 213.32 x^2 (1-x)^2 \times [1 - 2.9342 \sqrt{x(1-x)} + 2.2911 x(1-x)]$$

GPD overlap approach: pion case

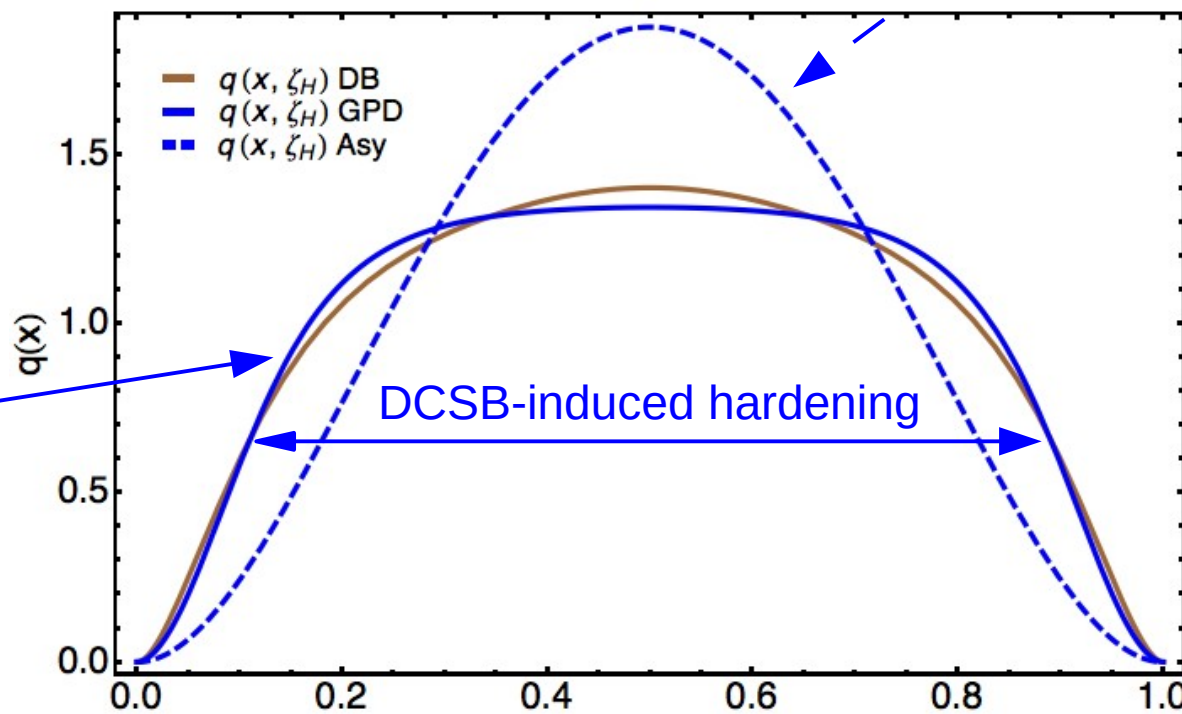
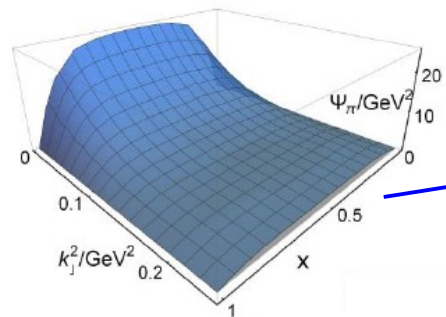
The overlap **valence-quark** GPD for a meson in the DGLAP kinematic region reads

$$H^q(x, \xi, t) = \int \frac{d^2\mathbf{k}_\perp}{16\pi^3} \Psi_{u\bar{f}}^*(x, \mathbf{k}_\perp) \Psi_{u\bar{f}}(x, \mathbf{k}_\perp) = q^\pi(x; \zeta_H)$$

Focus on the forward limit: the PDF that, in the overlap representation at low Fock space, can be expressed in terms of 2-body LFWFs at a given hadronic scale

$$q^\pi(x; \zeta_H) = 30x^2(1-x)^2$$

LFWF leading to asymptotic PDA



Direct computation of Mellin moments:

$$\langle x^m \rangle_{\zeta_H}^\pi = \int_0^1 dx x^m q^\pi(x; \zeta_H)$$

$$= \frac{N_c}{n \cdot P} \text{tr} \int_{dk} \left[\frac{n \cdot k_\eta}{n \cdot P} \right]^m \Gamma_\pi(k_\eta, P) S(k_\eta) n \cdot \partial_{k_\eta} [\Gamma_\pi(k_\eta, -P) S(k_\eta)]$$

M. Ding et al., PRD01(2020)054014

$$q^\pi(x; \zeta_H) = 213.32 x^2 (1-x)^2 \times [1 - 2.9342 \sqrt{x(1-x)} + 2.2911 x(1-x)]$$

GPD overlap approach: pion case

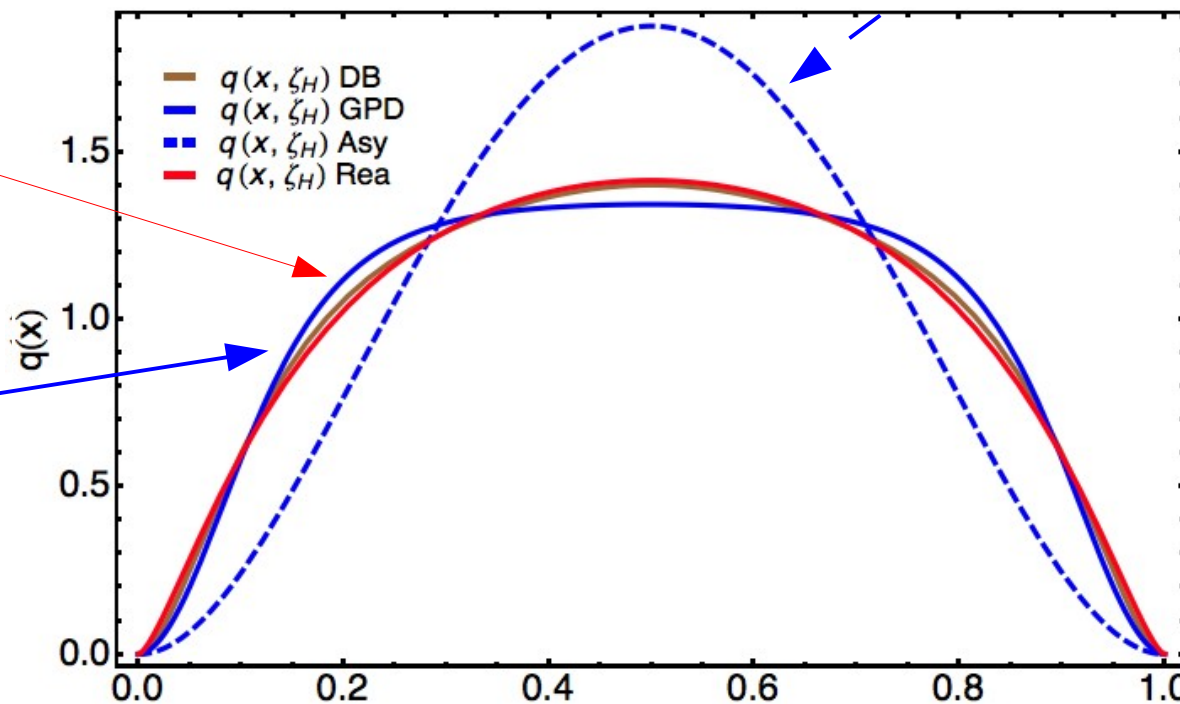
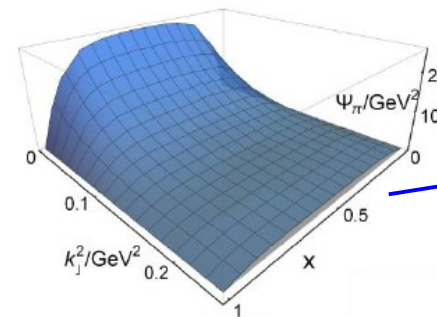
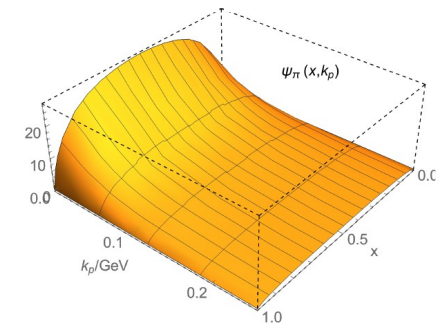
The overlap **valence-quark** GPD for a meson in the DGLAP kinematic region reads

$$H^q(x, \xi, t) = \int \frac{d^2\mathbf{k}_\perp}{16\pi^3} \Psi_{u\bar{f}}^*(x, \mathbf{k}_\perp) \Psi_{u\bar{f}}(x, \mathbf{k}_\perp) = q^\pi(x; \zeta_H)$$

Focus on the forward limit: the PDF that, in the overlap representation at low Fock space, can be expressed in terms of 2-body LFWFs at a given hadronic scale

$$q^\pi(x; \zeta_H) = 30x^2(1-x)^2$$

LFWF leading to asymptotic PDA



Direct computation of Mellin moments:

$$\langle x^m \rangle_{\zeta_H}^\pi = \int_0^1 dx x^m q^\pi(x; \zeta_H)$$

$$= \frac{N_c}{n \cdot P} \text{tr} \int_{dk} \left[\frac{n \cdot k_\eta}{n \cdot P} \right]^m \Gamma_\pi(k_\eta, P) S(k_\eta) n \cdot \partial_{k_\eta} [\Gamma_\pi(k_\eta, -P) S(k_\eta)]$$

M. Ding et al., PRD01(2020)054014

$$q^\pi(x; \zeta_H) = 213.32 x^2 (1-x)^2 \times [1 - 2.9342 \sqrt{x(1-x)} + 2.2911 x(1-x)]$$

Comparison with experiment: DGLAP evolution

A master equation for the (1-loop) moments' evolution:

$$\frac{d}{dt} q(x, t) = \frac{\alpha(t)}{4\pi} \int_x^1 \frac{dy}{y} q(y, t) P\left(\frac{x}{y}\right) + \dots$$

$$M_n(t) = \int_0^1 dx x^n q(x, t)$$

$$t = \ln\left(\frac{\xi^2}{\xi_0^2}\right)$$

Moments' evolution (1-loop):

$$\frac{d}{dt} M_n(t) = -\frac{\alpha(t)}{4\pi} \gamma_0^n M_n(t) + \dots$$

$$-\int_0^1 dx x^n P(x) = \gamma_0^n$$

$$P(x) = \frac{8}{3} \left(\frac{1+z^2}{(1-x)_+} + \frac{3}{2} \delta(x-1) \right)$$

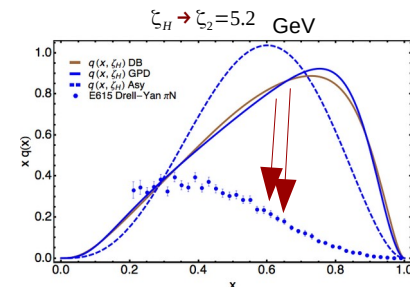
$$\frac{d}{dt} \alpha(t) = -\frac{\alpha^2(t)}{4\pi} \beta_0 + \dots$$

$$\gamma_0^n = -\frac{4}{3} \left(3 + \frac{2}{(n+2)(n+3)} - 4 \sum_{i=1}^{n+1} \frac{1}{i} \right)$$

$$\alpha(t) = \frac{4\pi}{\beta_0(t-t_\Lambda)} + \dots$$

$$t_\Lambda = \ln\left(\frac{\Lambda^2}{\xi_0^2}\right)$$

$$M_n(t) = M_n(t_0) \left(\frac{\alpha(t)}{\alpha(t_0)} \right)^{\gamma_0^n / \beta_0}$$



Comparison with experiment: DGLAP evolution

Which value of Lambda?

$$\alpha(t) = \frac{4\pi}{\beta_0(t-t_\Lambda)} + \dots = \frac{4\pi}{\beta_0 \ln\left(\frac{\xi^2}{\Lambda^2}\right)} + \dots$$

Comparison with experiment: DGLAP evolution

Which value of Lambda? It depends on the scheme... Indeed, at the one-loop level, its value defines by itself the scheme!!!

$$\alpha(t) = \frac{4\pi}{\beta_0(t-t_\Lambda)} + \dots = \frac{4\pi}{\beta_0 \ln\left(\frac{\xi^2}{\Lambda^2}\right)} + \dots$$

$$\ln\left(\frac{\Lambda^2}{\Lambda'^2}\right) = \frac{4\pi}{\beta_0} \left(\frac{1}{\alpha(t)} - \frac{1}{\bar{\alpha}(t)} \right) + \dots = \frac{4\pi c}{\beta_0}$$

$$\alpha(t) = \bar{\alpha}(t) (1 + c \bar{\alpha}(t) + \dots)$$



Comparison with experiment: **DGLAP evolution**

Which value of Lambda? It depends on the scheme... Indeed, at the one-loop level, its value defines by itself the scheme!!!

$$\alpha(t) = \frac{4\pi}{\beta_0(t-t_\Lambda)} + \dots = \frac{4\pi}{\beta_0 \ln\left(\frac{\xi^2}{\Lambda^2}\right)} + \dots$$

$$\alpha(t) = \bar{\alpha}(t)(1 + c \bar{\alpha}(t) + \dots)$$

$$\ln\left(\frac{\Lambda^2}{\Lambda'^2}\right) = \frac{4\pi}{\beta_0} \left(\frac{1}{\alpha(t)} - \frac{1}{\bar{\alpha}(t)} \right) + \dots = \frac{4\pi c}{\beta_0}$$

$$\frac{d}{dt} M_n(t) = -\frac{\alpha(t)}{4\pi} \gamma_0^n M_n(t) + \dots$$

$$\frac{d}{dt} \alpha(t) = -\frac{\alpha^2(t)}{4\pi} \beta_0 + \dots$$

The evolution will thus depend on the scheme *via* the perturbative truncation

Comparison with experiment: **DGLAP evolution**

$$\alpha(t) = \frac{4\pi}{\beta_0(t-t_\Lambda)} + \dots = \frac{4\pi}{\beta_0 \ln\left(\frac{\xi^2}{\Lambda^2}\right)} + \dots$$

$$\alpha(t) = \bar{\alpha}(t)(1 + c \bar{\alpha}(t) + \dots)$$

$$\ln\left(\frac{\Lambda^2}{\Lambda'^2}\right) = \frac{4\pi}{\beta_0} \left(\frac{1}{\alpha(t)} - \frac{1}{\bar{\alpha}(t)} \right) + \dots = \frac{4\pi c}{\beta_0}$$

$$\frac{d}{dt} M_n(t) = -\frac{\bar{\alpha}(t)}{4\pi} \gamma_0^n M_n(t) + \dots$$

$$\frac{d}{dt} \bar{\alpha}(t) = -\frac{\bar{\alpha}^2(t)}{4\pi} \beta_0 + \dots$$

The evolution will thus depend on the scheme *via* the perturbative truncation and the usual prejudice is that truncation errors are optimally small in MS scheme.

PDG2018:
[PRD98(2018)030001]

$$\Lambda_{MS}^{(5)} = (210 \pm 14) \text{ MeV}, \quad (9.24b)$$

$$\Lambda_{MS}^{(4)} = (292 \pm 16) \text{ MeV}, \quad (9.24c)$$

$$\Lambda_{MS}^{(3)} = (332 \pm 17) \text{ MeV}, \quad (9.24d)$$

Comparison with experiment: **DGLAP evolution**

Which value of Lambda? It depends on the scheme... Indeed, at the one-loop level, its value defines by itself the scheme!!!

$$\alpha(t) = \frac{4\pi}{\beta_0(t-t_\Lambda)} + \dots = \frac{4\pi}{\beta_0 \ln\left(\frac{\xi^2}{\Lambda^2}\right)} + \dots$$

$$\alpha(t) = \bar{\alpha}(t)(1 + c \bar{\alpha}(t) + \dots)$$

$$\ln\left(\frac{\Lambda^2}{\bar{\Lambda}^2}\right) = \frac{4\pi}{\beta_0} \left(\frac{1}{\alpha(t)} - \frac{1}{\bar{\alpha}(t)} \right) + \dots = \frac{4\pi c}{\beta_0}$$

$$\frac{d}{dt} M_n(t) = -\frac{\alpha(t)}{4\pi} \gamma_0^n M_n(t) + \dots$$

$$\frac{d}{dt} \alpha(t) = -\frac{\alpha^2(t)}{4\pi} \beta_0 + \dots$$

The evolution will thus depend on the scheme *via* the perturbative truncation

The use of $\Lambda = 0.234$ GeV can be thus interpreted as the choice of a particular scheme, differing from MS.

Comparison with experiment: **DGLAP evolution**

Which value of Lambda? It depends on the scheme... Indeed, at the one-loop level, its value defines by itself the scheme!!!

$$\alpha(t) = \frac{4\pi}{\beta_0(t-t_\Lambda)} + \dots = \frac{4\pi}{\beta_0 \ln\left(\frac{\xi^2}{\Lambda^2}\right)} + \dots$$

$$\alpha(t) = \bar{\alpha}(t) (1 + c \bar{\alpha}(t) + \dots)$$

$$\ln\left(\frac{\Lambda^2}{\bar{\Lambda}^2}\right) = \frac{4\pi}{\beta_0} \left(\frac{1}{\alpha(t)} - \frac{1}{\bar{\alpha}(t)} \right) + \dots = \frac{4\pi c}{\beta_0}$$

$$\frac{d}{dt} M_n(t) = -\frac{\alpha(t)}{4\pi} \gamma_0^n M_n(t)$$

The evolution will thus depend on the scheme *via* the perturbative truncation

The use of $\Lambda = 0.234 \text{ GeV}$ can be thus interpreted as the choice of a particular scheme, differing from MS. **Beyond this, the scheme can be defined in such a way that one-loop DGLAP is exact at all orders (Grunberg's effective charge).**

Comparison with experiment: **DGLAP evolution**

Which value of Lambda? It depends on the scheme... Indeed, at the one-loop level, its value defines by itself the scheme!!!

$$\alpha(t) = \frac{4\pi}{\beta_0(t-t_\Lambda)} + \dots = \frac{4\pi}{\beta_0 \ln\left(\frac{\xi^2}{\Lambda^2}\right)} + \dots$$

$$\alpha(t) = \bar{\alpha}(t) (1 + c \bar{\alpha}(t) + \dots)$$

$$\ln\left(\frac{\Lambda^2}{\bar{\Lambda}^2}\right) = \frac{4\pi}{\beta_0} \left(\frac{1}{\alpha(t)} - \frac{1}{\bar{\alpha}(t)} \right) + \dots = \frac{4\pi c}{\beta_0}$$

$$\frac{d}{dt} M_n(t) = -\frac{\alpha(t)}{4\pi} \gamma_0^n M_n(t)$$

The evolution will thus depend on the scheme *via* the perturbative truncation

$$\frac{d}{dt} q(x, t) = \frac{\alpha(t)}{4\pi} \int_x^1 \frac{dy}{y} q(y, t) P\left(\frac{x}{y}\right)$$

The use of $\Lambda = 0.234$ GeV can be thus interpreted as the choice of a particular scheme, differing from MS. **Beyond this, the scheme can be defined in such a way that one-loop DGLAP is exact at all orders (Grunberg's effective charge).**

Comparison with experiment: PI effective charge

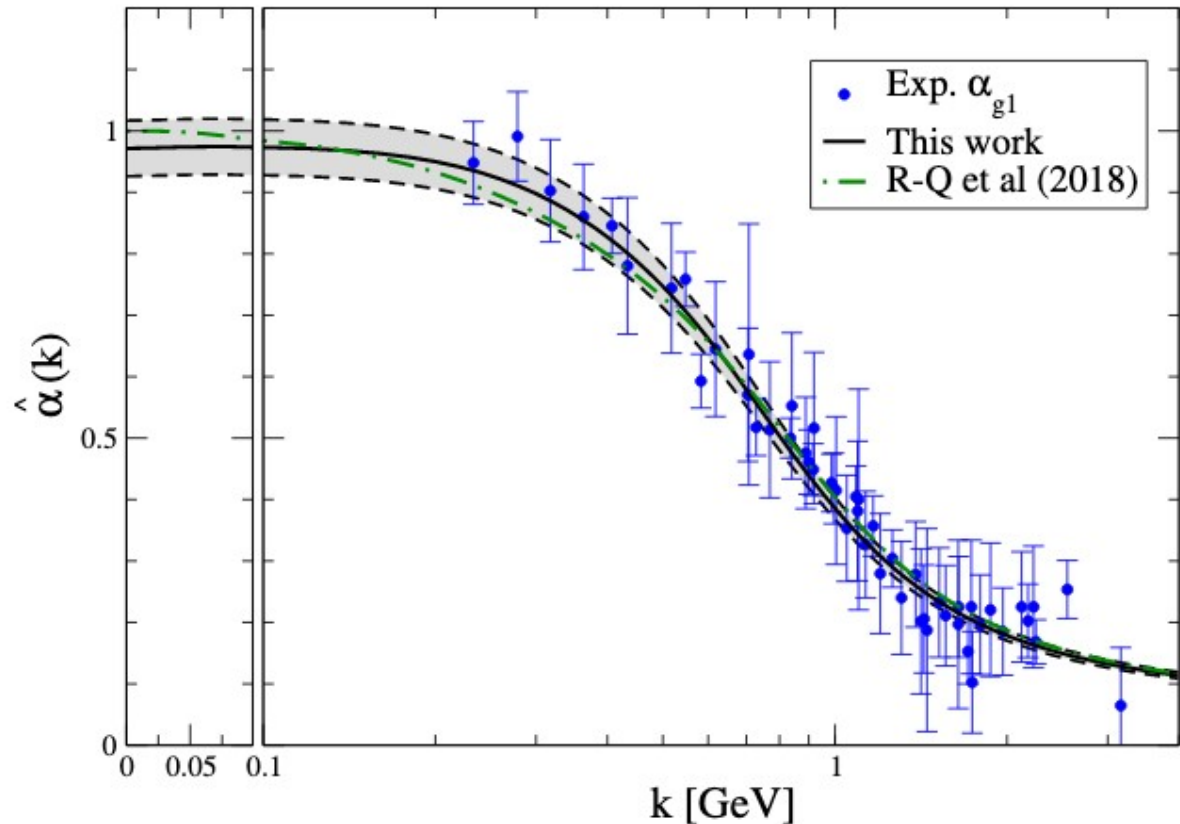
D.B et al., PRD96(2017)054026

J.R-Q et al., FBS59(2018)121

Z-F Cui et al., arXiv:1912.08232

Process-independent charge, defined as an analogue of the QED Gell-Mann-Low, on the basis of the PT-BFM truncation of DSEs in the gluon sector

Gauge-independent, no Landau pole, fully determined by the gluon sector, known to unify a wide range of observables, it compares very well with the Bjorken sum rule charge...



It emerges as a strong candidate to represent the interaction strength of QCD at any scale

Assumption: PI effective charge corresponds with the effective charge for the PDF evolution

$m_0 = 0.43(1)$ GeV emerges as natural nonperturbative scale marking the boundary between soft and hard physics, thus ensuring that parton modes are screened from interaction

$$\zeta_H = m_0$$

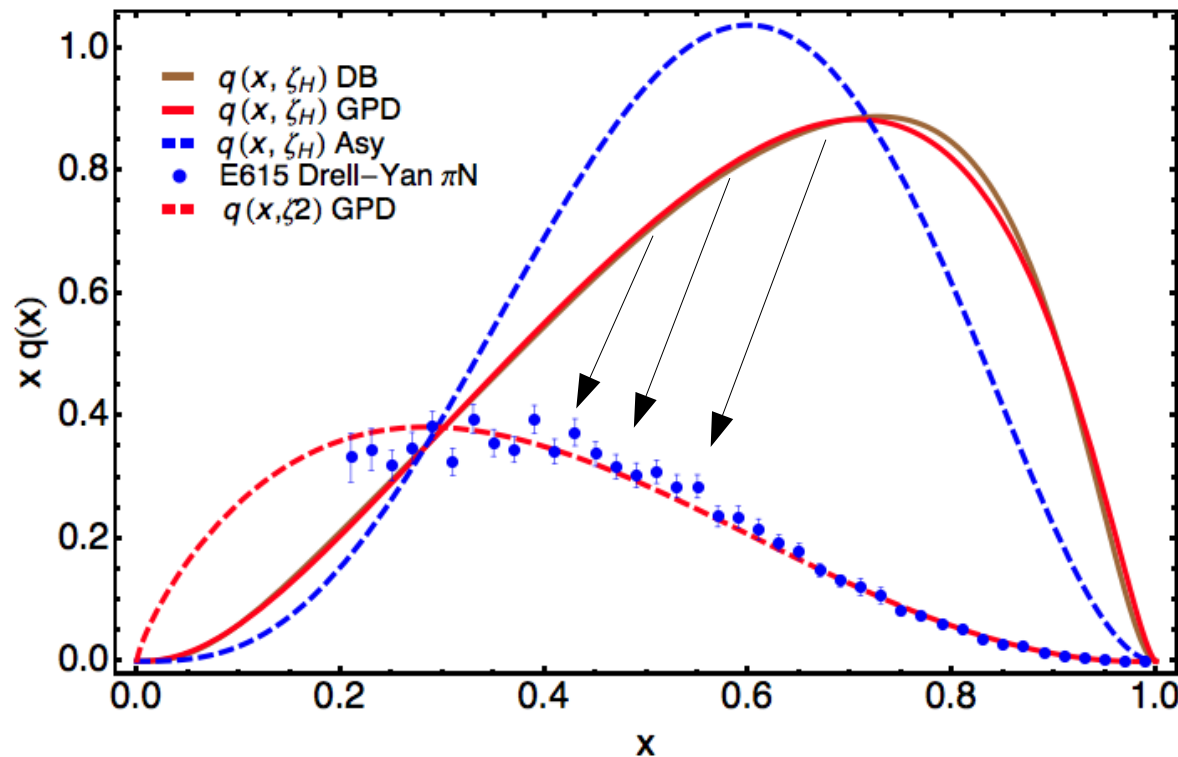
Comparison with experiment:

Then, one can evolve the pion PDF, by using one-loop DGLAP evolution and the effective charge, from the hadronic scale up to the relevant one for the E615 experiment:

$$M_n(t) = M_n(t_0) \exp\left(-\frac{\gamma_0^n}{4\pi} \int_{t_0}^t dz \alpha(z)\right)$$

[Aicher et al., PRL105(2010)252003]

$$\zeta_H \equiv m_0 \rightarrow \zeta_2 = 5.2 \text{ GeV}$$



After identifying $m_0 \equiv \zeta_H$, all the scales (and the evolution between them) appear thus fixed. **And the agreement with E615 data is perfect!!!**

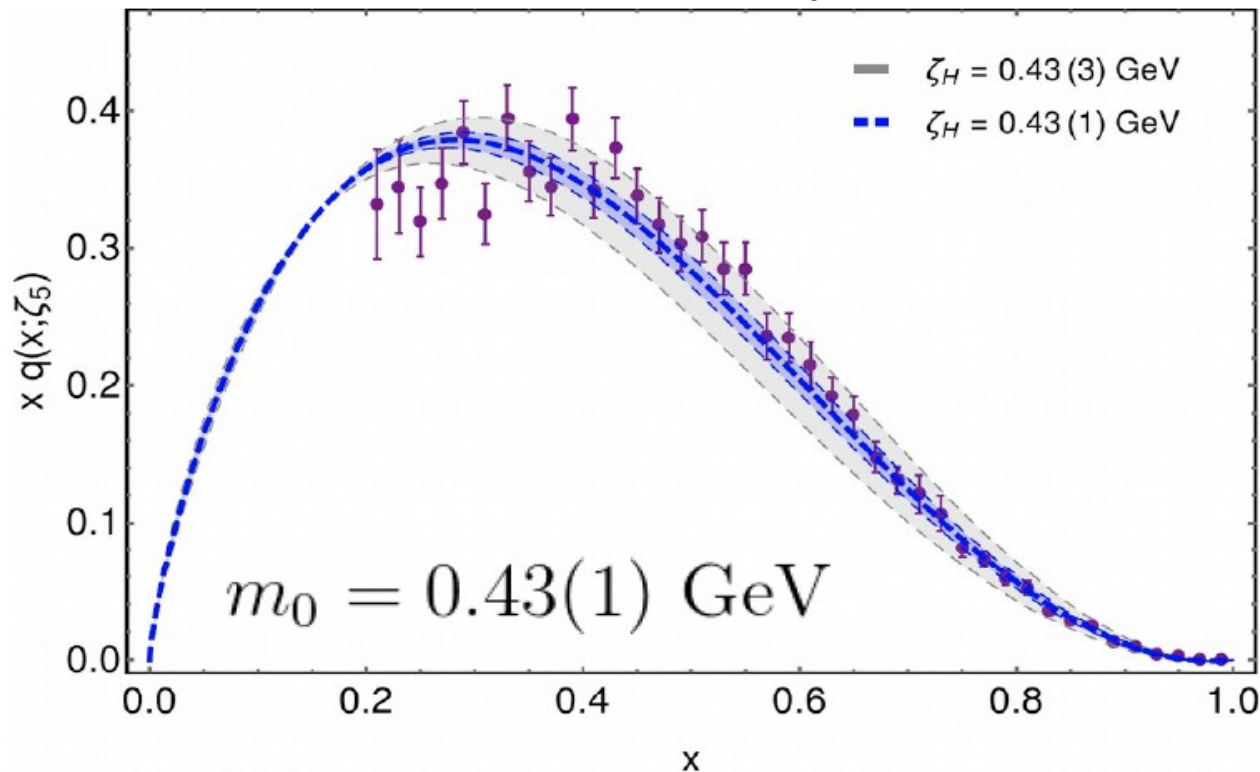
Comparison with experiment:

Then, one can evolve the pion PDF, by using one-loop DGLAP evolution and the effective charge, from the hadronic scale up to the relevant one for the E615 experiment:

$$M_n(t) = M_n(t_0) \exp\left(-\frac{\gamma_0^n}{4\pi} \int_{t_0}^t dz \alpha(z)\right)$$

[Aicher et al., PRL105(2010)252003]

$$\zeta_H \equiv m_0 \rightarrow \zeta_2 = 5.2 \text{ GeV}$$



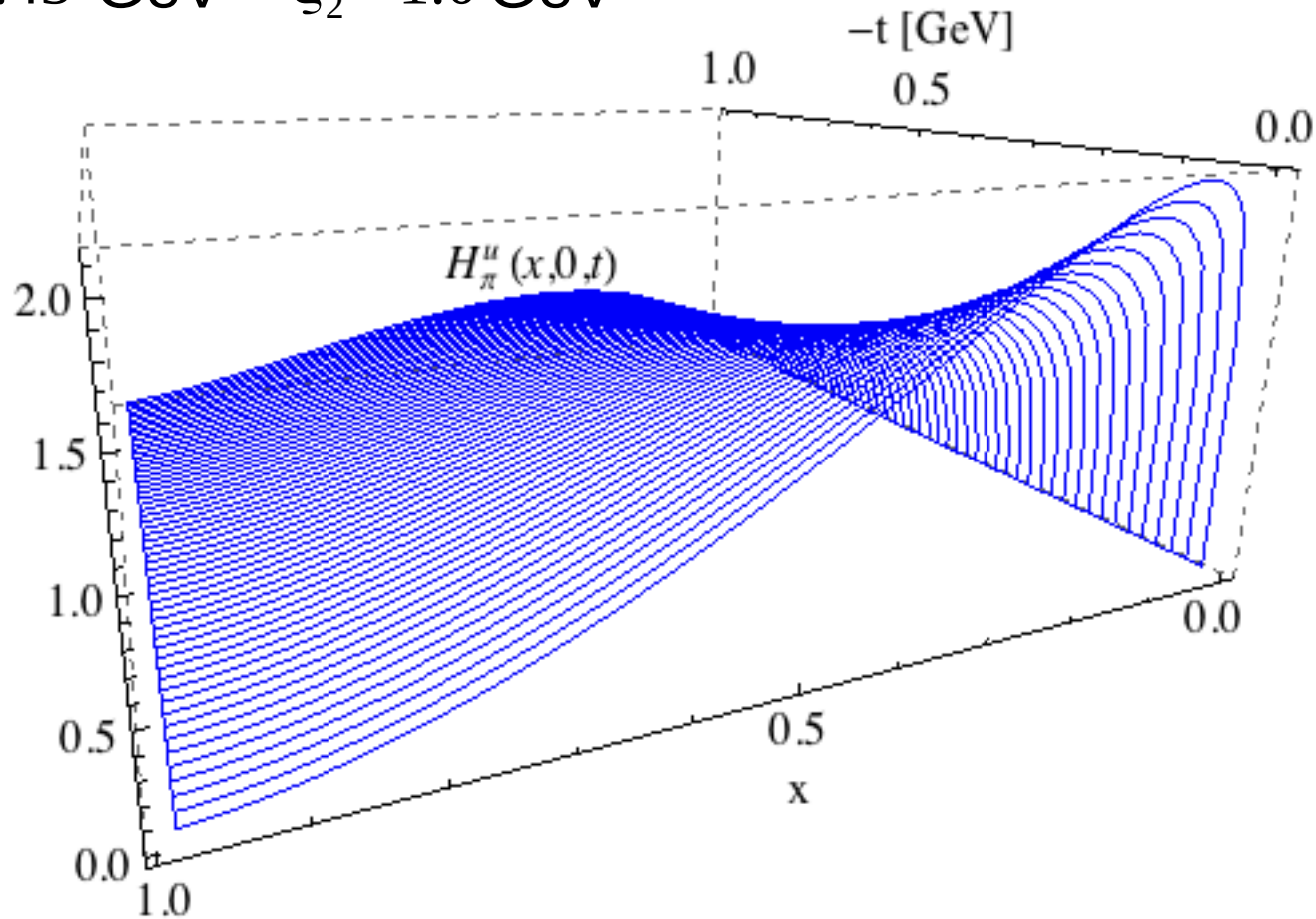
After identifying $m_0 \equiv \zeta_H$, all the scales (and the evolution between them) appear thus fixed. **And the agreement with E615 data is perfect!!!**

GPD overlap approach: pion case

The overlap **valence-quark** GPD for a meson in the DGLAP kinematic region reads

$$H^q(x, \xi, t) = \int \frac{d^2\mathbf{k}_\perp}{16\pi^3} \Psi_{u\bar{f}}^* \left(\frac{x-\xi}{1-\xi}, \mathbf{k}_\perp + \frac{1-x}{1-\xi} \frac{\Delta_\perp}{2} \right) \Psi_{u\bar{f}} \left(\frac{x+\xi}{1+\xi}, \mathbf{k}_\perp - \frac{1-x}{1+\xi} \frac{\Delta_\perp}{2} \right)$$

$$\zeta_0 = \zeta_H = 0.43 \text{ GeV} \rightarrow \zeta_2 = 1.0 \text{ GeV}$$



Singlet components evolution

Let us also consider the singlet components:
(an almost textbook exercise)

$$\gamma_{0,AB}^{S,(m)} = - \int_0^1 dx x^m P_{0,AB}^S(x)$$

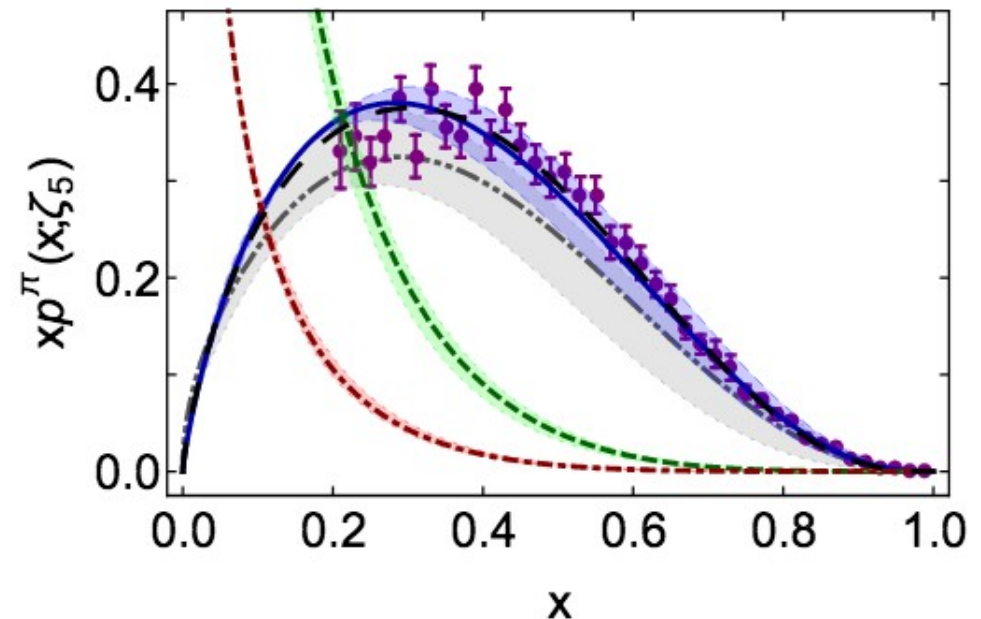
$$\zeta^2 \frac{d}{d\zeta^2} P^{-1} \begin{pmatrix} M_q^{(m)}(\zeta) \\ M_G^{(m)}(\zeta) \end{pmatrix} = - \frac{\alpha(\zeta^2)}{4\pi} \Gamma_D^{(m)} P^{-1} \begin{pmatrix} M_q^{(m)}(\zeta_H) \\ 0 \end{pmatrix}$$

$$P^{-1} \Gamma_0^{S,(m)} P = \begin{pmatrix} \lambda_+^{(m)} & 0 \\ 0 & \lambda_-^{(m)} \end{pmatrix}$$

Initial conditions at the hadronic scale, where only valence-quarks are assumed to be the correct degrees-of-freedom, can be evolved and shown to produce non-zero gluon and sea-quark components.

ζ_5	$\langle x \rangle_u^\pi$	$\langle x^2 \rangle_u^\pi$	$\langle x^3 \rangle_u^\pi$
Ref. [31]	0.17(1)	0.060(9)	0.028(7)
Herein	0.21(2)	0.076(9)	0.036(5)

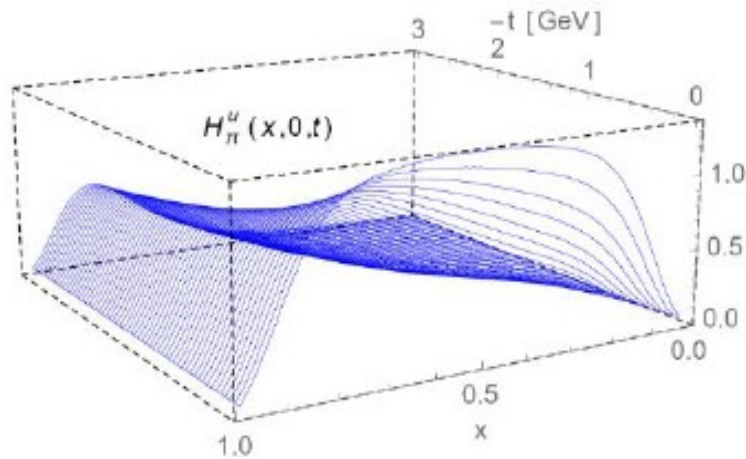
$$\langle x \rangle_g^\pi = 0.45(1), \quad \langle x \rangle_{\text{sea}}^\pi = 0.14(2).$$



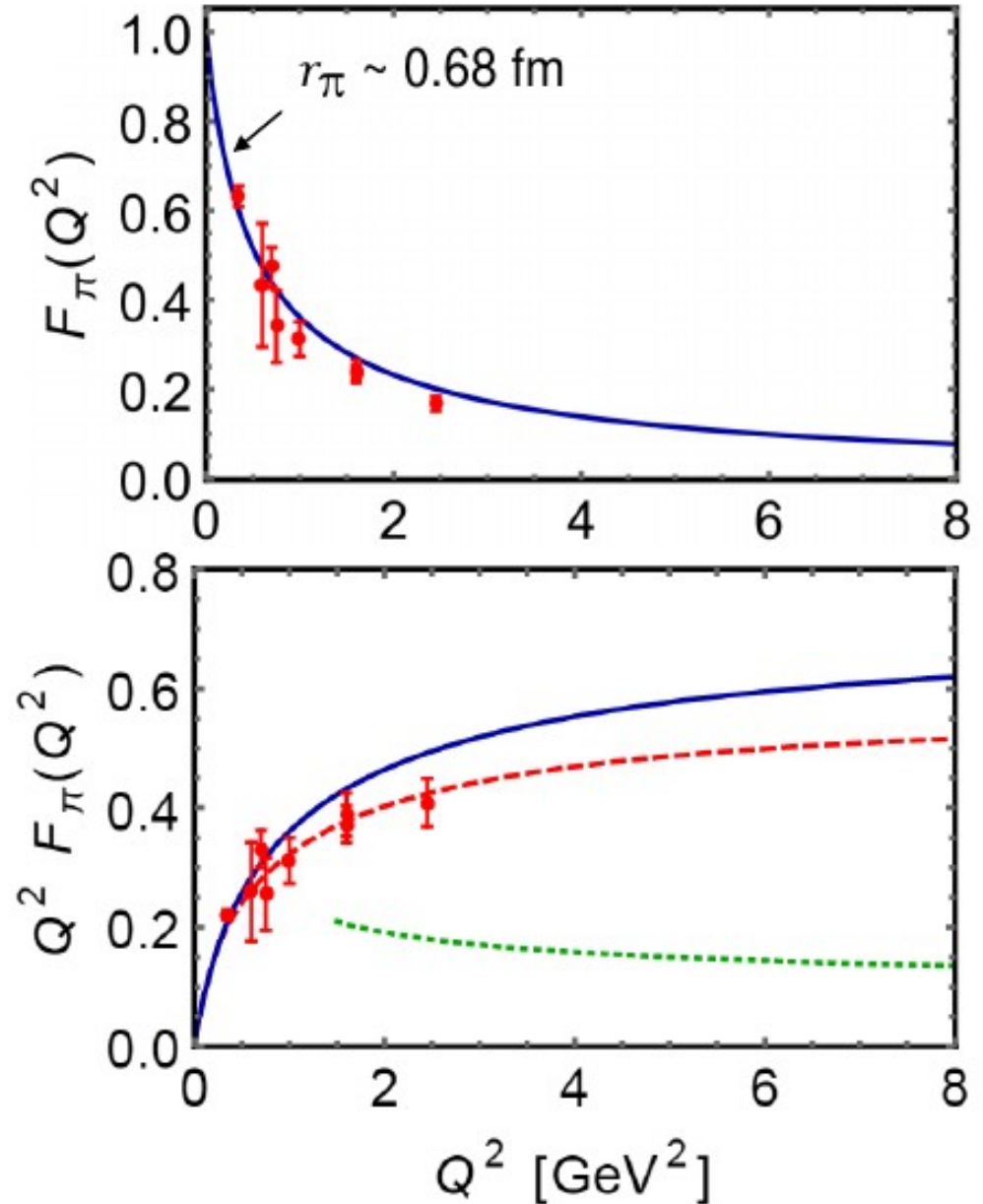
Pion realistic picture: Electromagnetic Form Factor

$$F_M(\Delta^2) = e_u F_M^u(\Delta^2) + e_f F_M^f(\Delta^2), \quad F_M^q(-t = \Delta^2) = \int_{-1}^1 dx H_M^q(x, \xi, t)$$

↙ Electric charges ↘

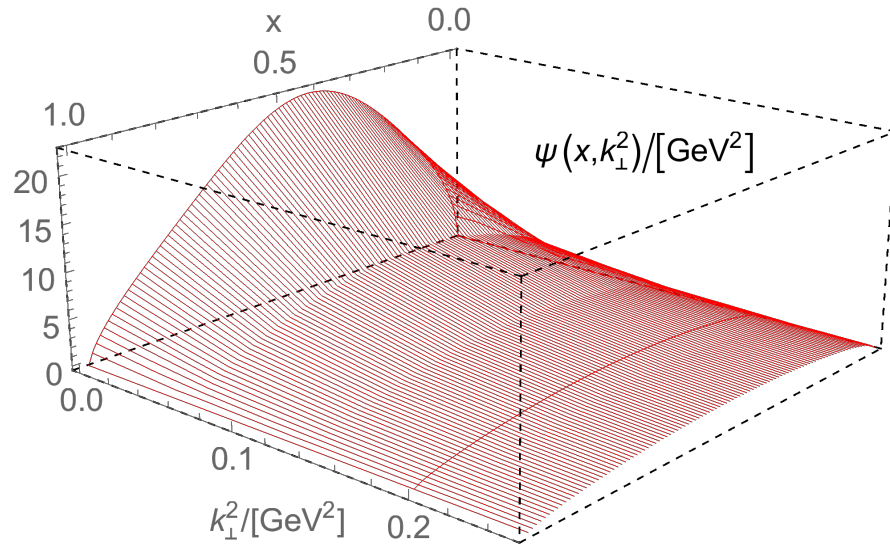


- Blue:** Computed from GPD
- Green:** Computed from HS formula
- Red:** 'Evolved' form factor

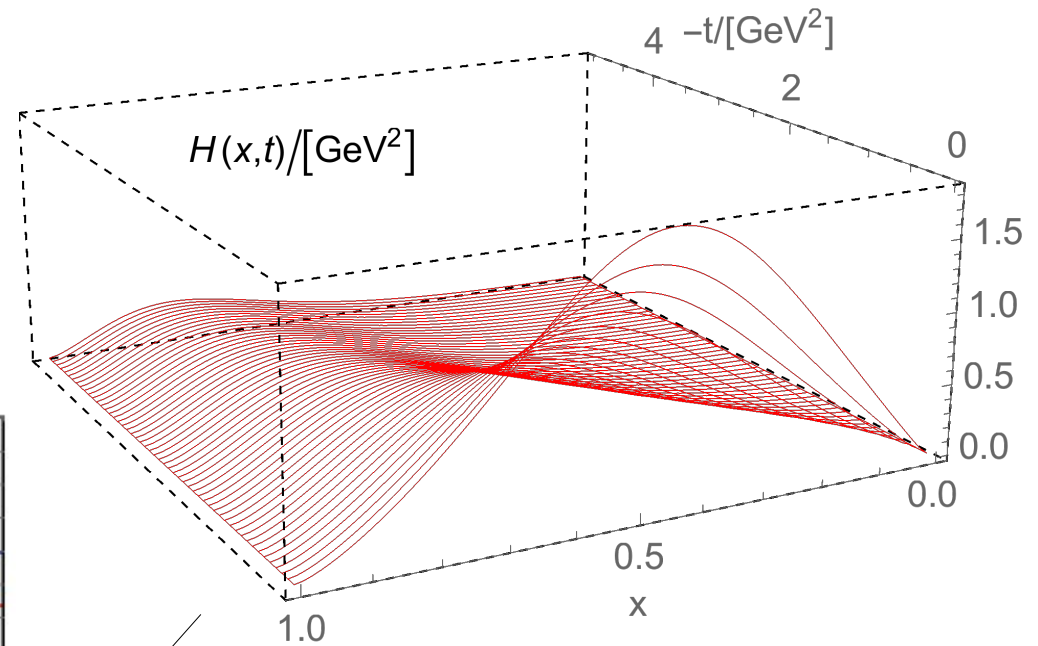


Kaon preliminary results:

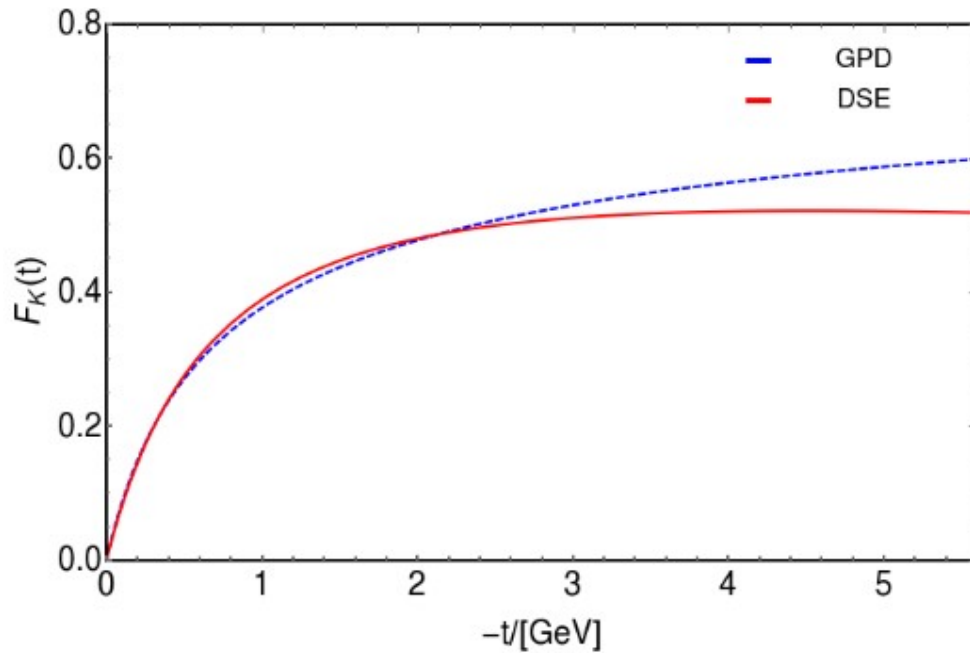
Identifying first the LFWF (see Khépani's talk)



one obtains the DGLAP GPD:



and the electromagnetic form factor.



A word about gravitational form factors:

First, polynomiality:

$$\int_{-1}^1 dx x^m H(x, \xi, t) = \sum_{k=0}^{m+1} C_k^{(m)}(t) \xi^k \quad (\text{Time reversal symmetry implies } k \text{ even})$$

If one defines a function D such that:

$$\int_{-1}^1 dx x^m D(x, t) = C_{m+1}^m(t)$$

where $D(x, t) = 0 \quad \forall x \in [-\infty, -1) \cup (1, \infty]$

$$\int_{-1}^1 dx x^m \left(H(x, \xi, t) - \text{sign}(\xi) D\left(\frac{x}{\xi}\right) \right) = \sum_{k=0}^m C_k^{(m)}(t) \xi^k$$

$$\int_{\Omega} d\beta d\alpha h_{PW}(\beta, \alpha; t) \delta(x - \beta - \alpha\xi) = \mathcal{R}[h_{PW}]$$

$$\frac{1}{|\xi|} D\left(\frac{x}{\xi}, t\right) = \int_{\Omega} d\beta d\alpha \delta(\beta) D(\alpha, t) \delta(x - \beta - \alpha\xi) = \mathcal{R}[\delta D] \quad \begin{array}{l} \text{PW D-term} \\ \text{(Pure ERBL contribution)} \end{array}$$

Specializing for the case $m=1$

$$\int_{-1}^1 dx x H(x, \xi, t) = c_0^{(1)}(t) + \xi^2 \int_{-1}^1 dz z D(z, t)$$

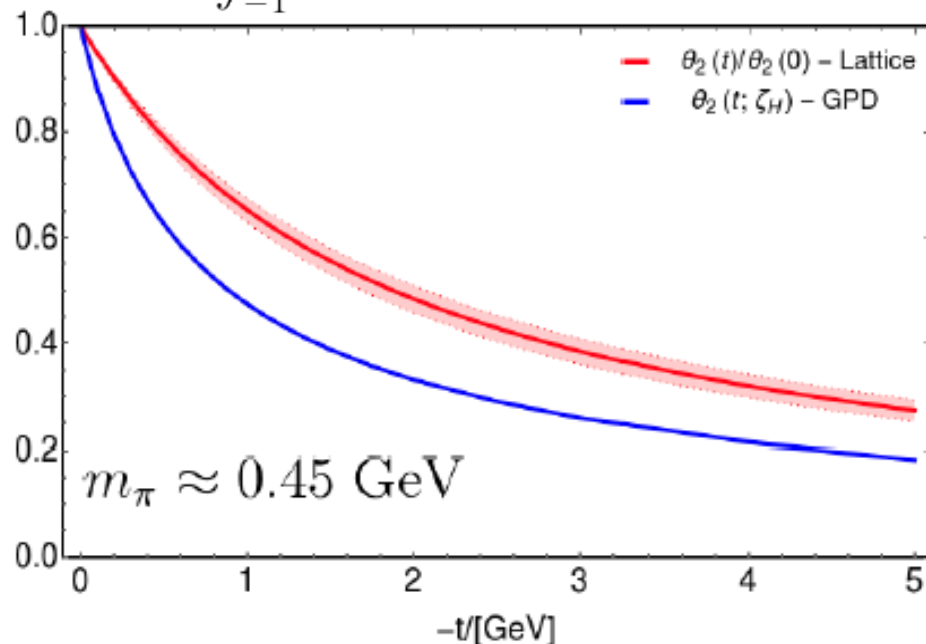
A word about gravitational form factors:

$$\int_{-1}^1 dx x H(x, \xi, t) = c_0^{(1)}(t) + \xi^2 \int_{-1}^1 dz z D(z, t)$$

Isospin-symmetric limit

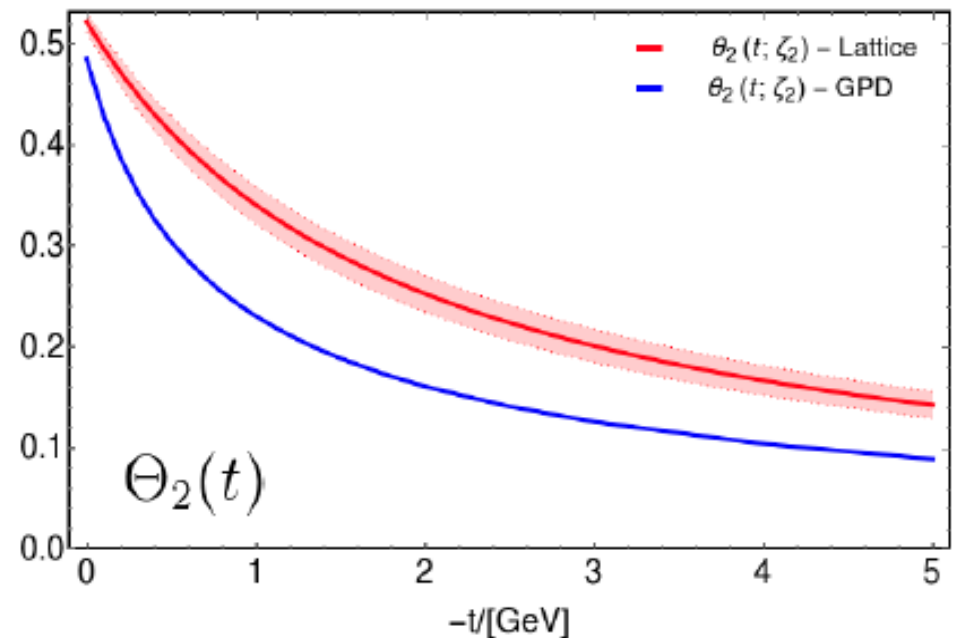
$$\frac{1}{2}\theta_2(t)$$

$$\theta_2(t) = \int_{-1}^1 dx x (H_{\pi^+}^u(x, 0, t) + H_{\pi^+}^d(-x, 0, t))$$



Lattice: (2007) Brömmel's dissertation.

GPD + Ding et al.



$$\Theta_2(0)/2 = \langle x \rangle = 0.261(5)$$

$$\Theta_2(0)/2 = \langle x \rangle = 0.242(20)$$

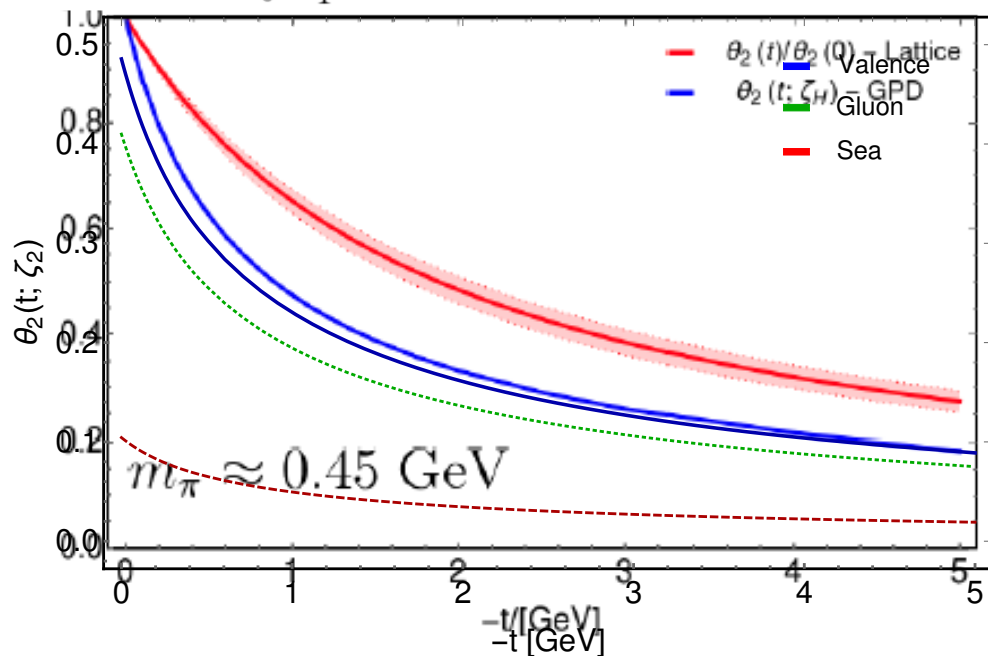
A word about gravitational form factors:

$$\int_{-1}^1 dx x H(x, \xi, t) = c_0^{(1)}(t) + \xi^2 \int_{-1}^1 dz z D(z, t)$$

Isospin-symmetric limit

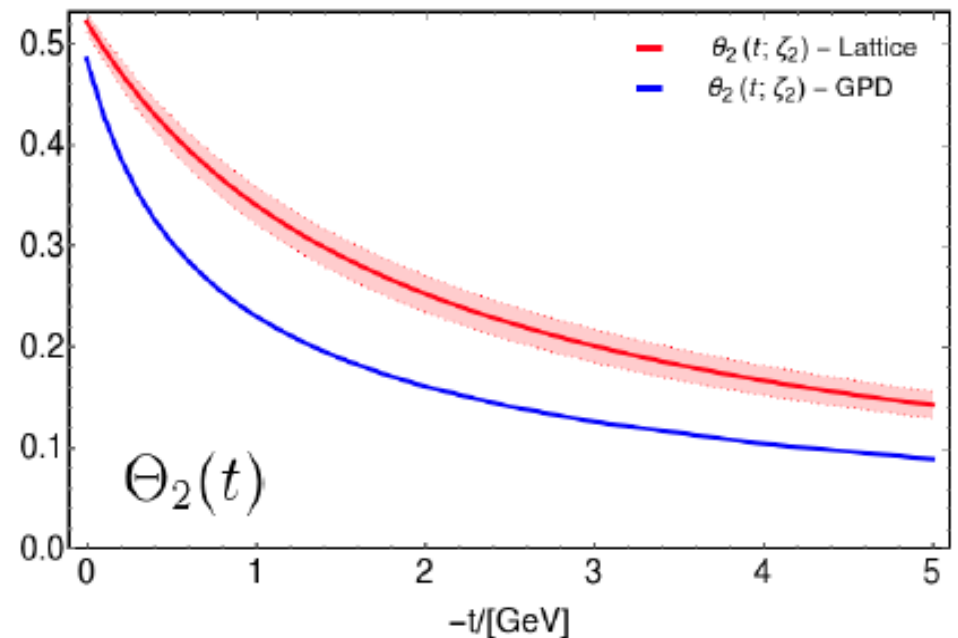
$$\frac{1}{2} \theta_2(t)$$

$$\theta_2(t) = \int_{-1}^1 dx x (H_{\pi^+}^u(x, 0, t) + H_{\pi^+}^d(-x, 0, t))$$



Lattice: (2007) Brömmel's dissertation.

GPD + Ding et al.



$$\Theta_2(0)/2 = \langle x \rangle = 0.261(5)$$

$$\Theta_2(0)/2 = \langle x \rangle = 0.242(20)$$

A word about gravitational form factors:

$$\int_{-1}^1 dx x H(x, \xi, t) = c_0^{(1)}(t) + \xi^2 \int_{-1}^1 dz z D(z, t)$$

$$\theta_2(t) = \int_{-1}^1 dx x (H_{\pi^+}^u(x, 0, t) + H_{\pi^+}^d(-x, 0, t))$$

3/2-Gegenbauer expansion

$$D(z, t) = (1 - z^2) \sum_{k=1, \text{odd}}^{\infty} d_k(t) C_k^{(3/2)}(x)$$

$$\frac{4}{5} d_1(t)$$

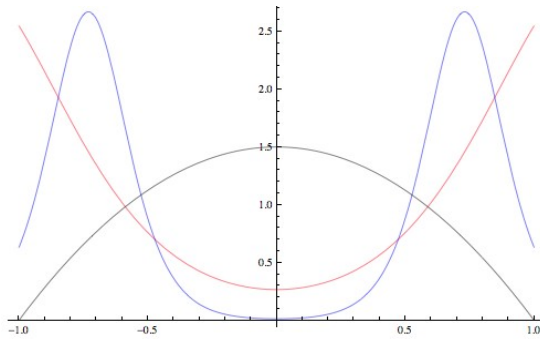
Only the first coefficient is needed!

LFWF + overlap approach cannot give access to the second gravitational moment. The Radon transform inversion of the DGLAP GPD cannot either (as it is nothing but a D-term contribution).

A possible way-out is considering unsubtracted t-channel dispersion relations to provide with a representation of the D-term form factor

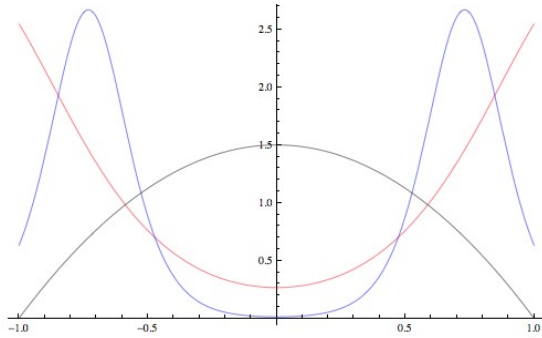
[See Pasquini et al., PLB739(2014)133, precisely determining $d_1(t)$ for a nucleon case]

Conclusions



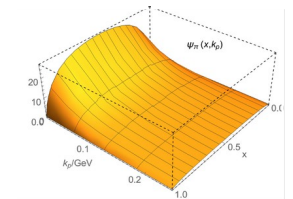
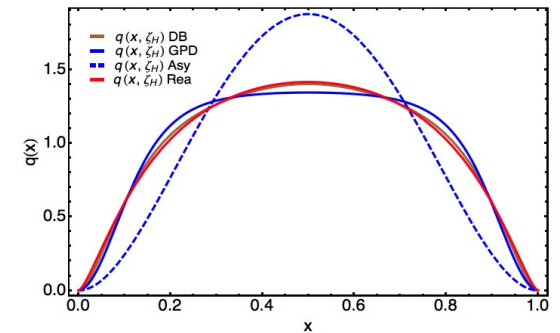
Owing to a sensible parametrisation of the BSA grounded on the so-called Nakanishi representation, one is left with a flexible algebraic model for the LFWF in terms of a **spectral density**.

Conclusions

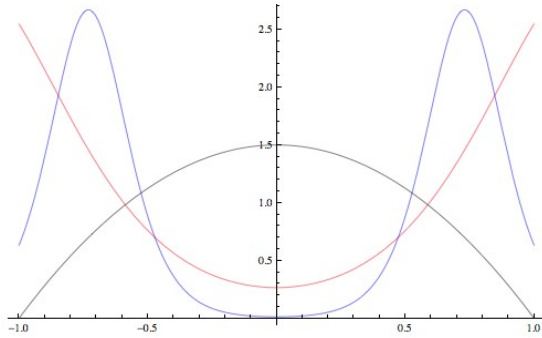


Owing to a sensible parametrisation of the BSA grounded on the so-called Nakanishi representation, one is left with a flexible algebraic model for the LFWF in terms of a **spectral density**.

A direct calculation of the PDF from realistic quark gap and Bethe-Salpeter equations' solutions (in the forward kinematical limit) delivers a benchmark result to identify the **spectral density** which corresponds to the **realistic LFWF**.

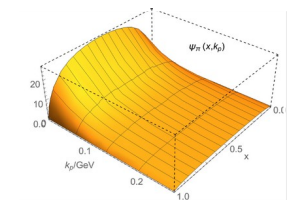
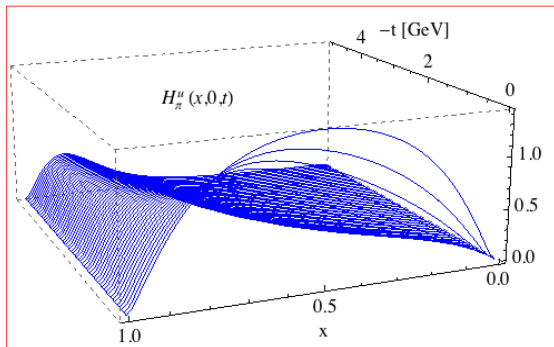
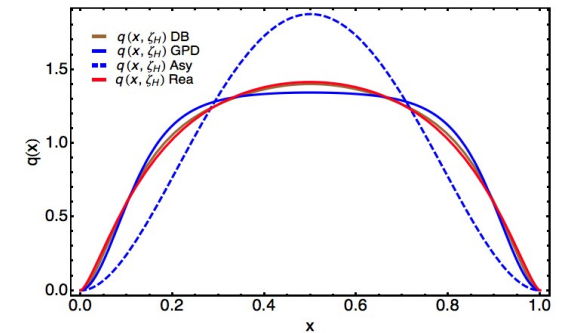


Conclusions



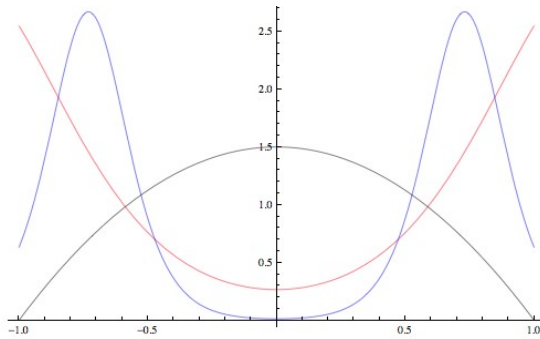
Owing to a sensible parametrisation of the BSA grounded on the so-called Nakanishi representation, one is left with a flexible algebraic model for the LFWF in terms of a **spectral density**.

A direct calculation of the PDF from realistic quark gap and Bethe-Salpeter equations' solutions (in the forward kinematical limit) delivers a benchmark result to identify the **spectral density** which corresponds to the **realistic LFWF**.



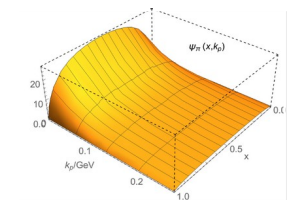
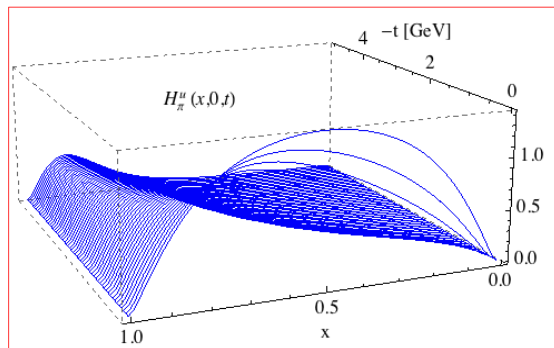
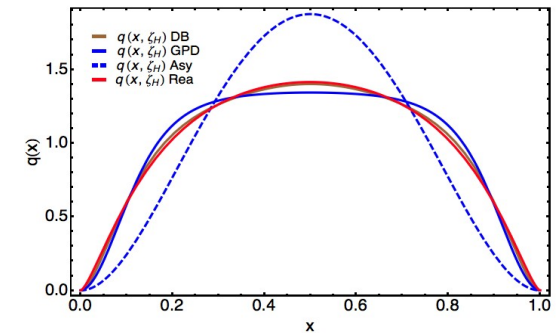
The overlap representation provides with a simple way to calculate **beyond the forward kinematic limit**, and thus obtain the GPD, although only in the **DGLAP region**.

Conclusions



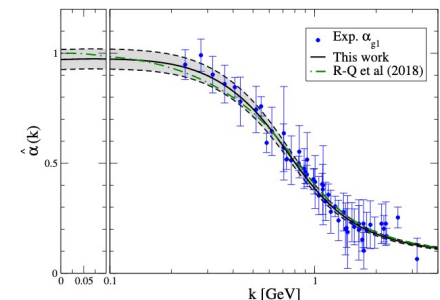
Owing to a sensible parametrisation of the BSA grounded on the so-called Nakanishi representation, one is left with a flexible algebraic model for the LFWF in terms of a **spectral density**.

A direct calculation of the PDF from realistic quark gap and Bethe-Salpeter equations' solutions (in the forward kinematical limit) delivers a benchmark result to identify the **spectral density** which corresponds to the **realistic LFWF**.

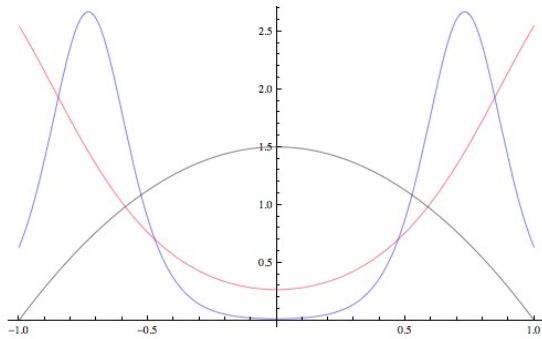


The overlap representation provides with a simple way to calculate **beyond the forward kinematic limit**, and thus obtain the GPD, although only in the **DGLAP region**.

A recently proposed **PI effective charge** can be used to make the DGLAP GPD evolve from the **hadronic scale** (where quasi-particle DSE's solutions are the correct degrees-of-freedom) up to any other relevant scale.



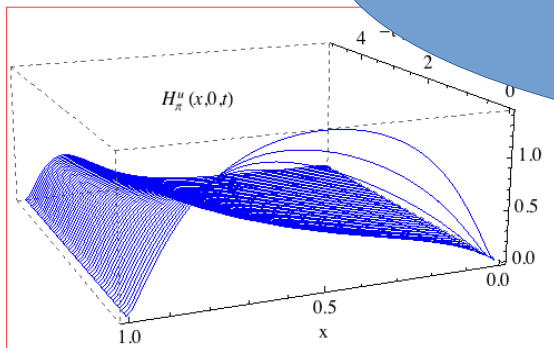
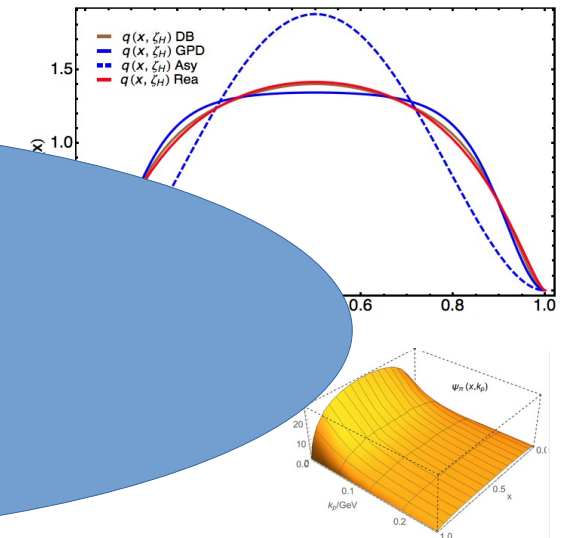
Conclusions



Owing to a sensible parametrisation of the BSA grounded on the so-called Nakanishi representation, one is left with a flexible algebraic model for the LFWF in terms of a **spectral density**.

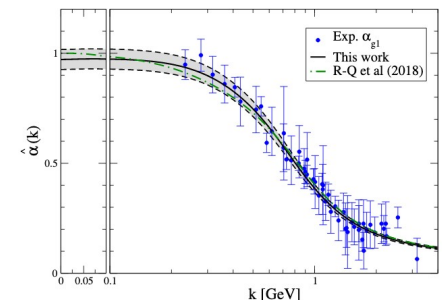
A direct calculation of the PDFs from the Bethe-Salpeter equation (in the forward kinematical limit) **spectral density**

Thank you!!



The overlap representation provides with a simple way to calculate **beyond the forward kinematic limit**, and thus obtain the GPD, although only in the **DGLAP region**.

A recently proposed **PI effective charge** can be used to make the DGLAP GPD evolve from the **hadronic scale** (where quasi-particle DSE's solutions are the correct degrees-of-freedom) up to any other relevant scale.



Backslides

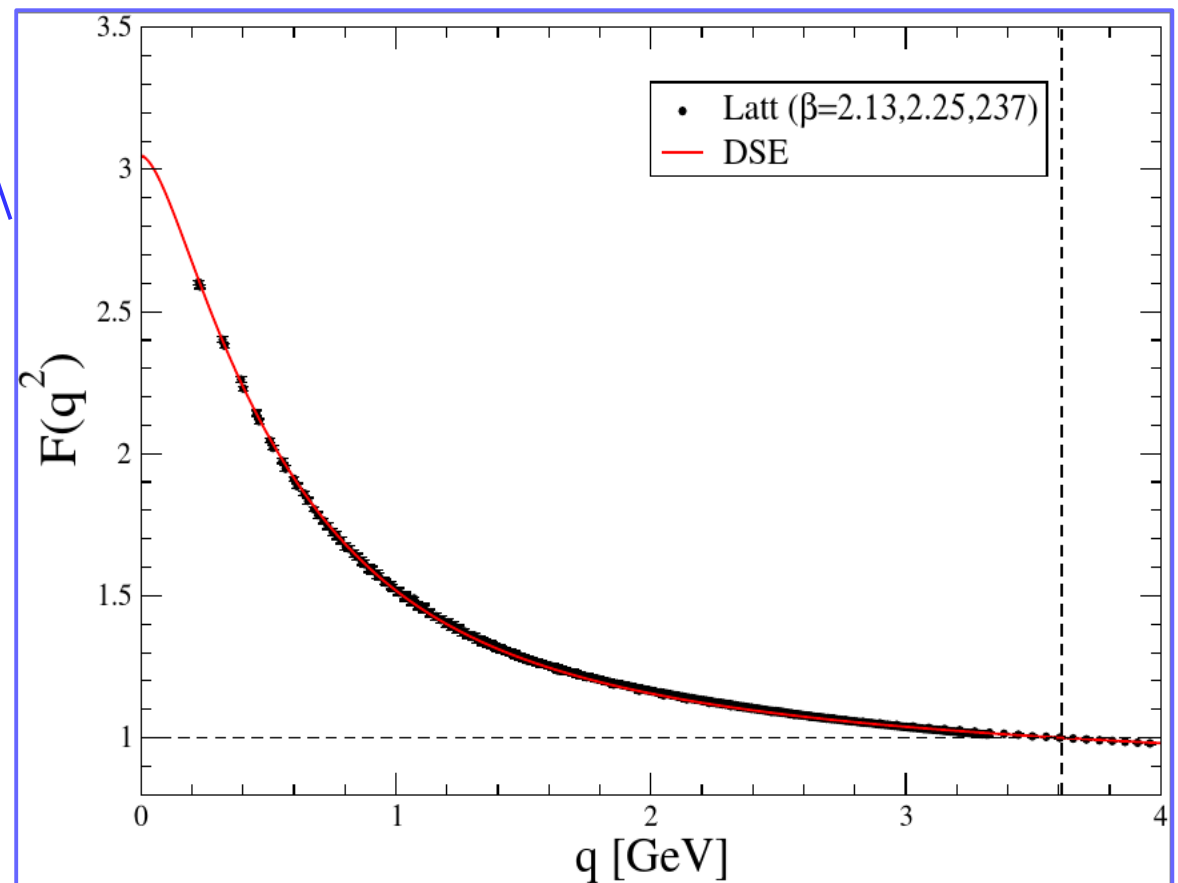
PI-effective charge from lattice data with Nf=3 flavors at the physical point

Preliminary results:

$$\hat{\alpha}_{\text{PI}}(q^2) = \frac{\hat{d}(q^2)}{\mathcal{D}(q^2)} \simeq \frac{\alpha_T(q^2)}{q^2 [1 - L(q^2, \zeta^2)F(q^2, \zeta^2)]^2} \frac{m_0^2 \Delta_F(0, \zeta^2)}{\Delta_F(q^2, \zeta^2)}$$
$$= \alpha_T(\zeta^2) \frac{F(q^2, \zeta^2)}{[1 - L(q^2, \zeta^2)F(q^2, \zeta^2)]^2} \Delta_F(0, \zeta^2) m_0^2$$

The IR running of the PI effective charge with momenta only depends on:

- The ghost dressing function



PI-effective charge from lattice data with Nf=3 flavors at the physical point

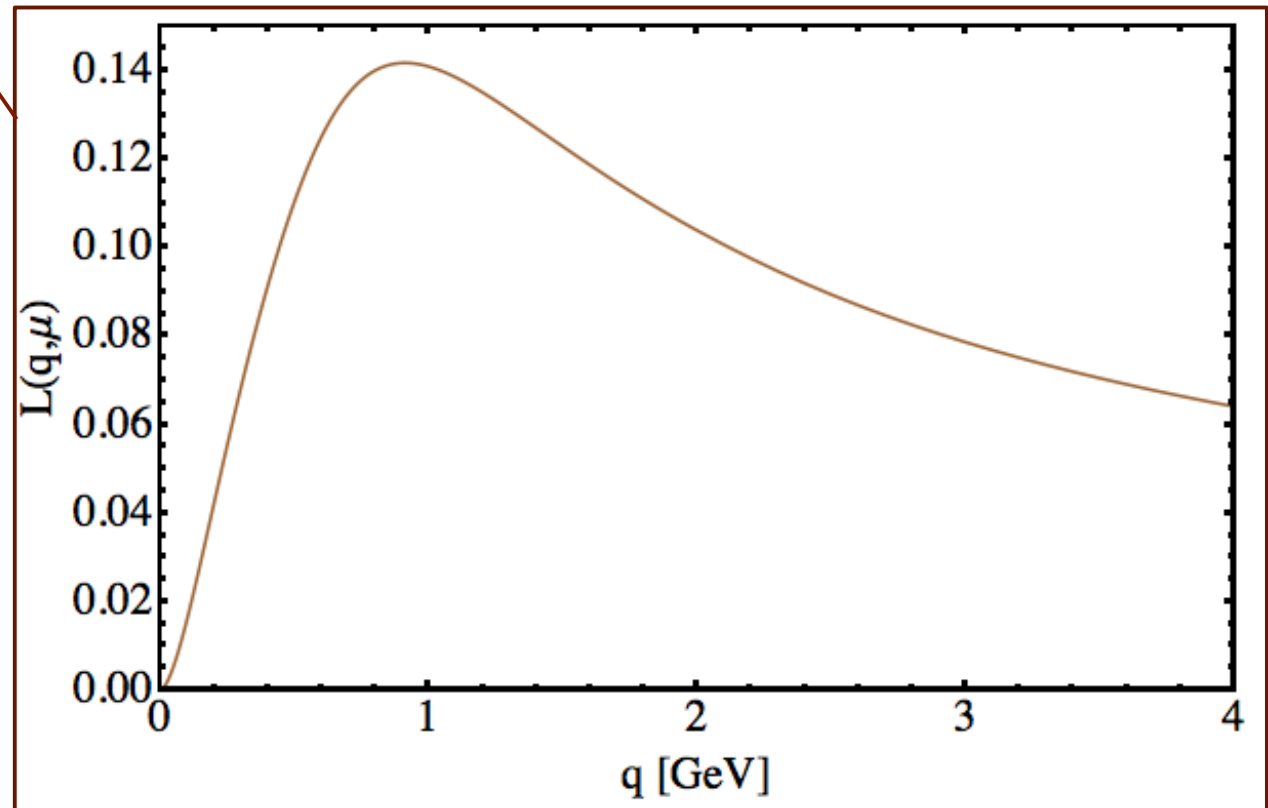
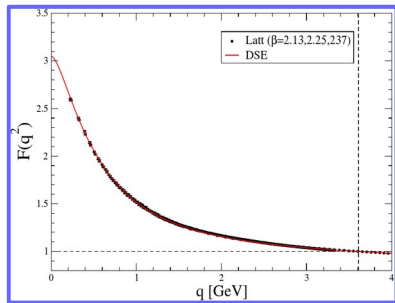
Preliminary results:

$$\hat{\alpha}_{\text{PI}}(q^2) = \frac{\hat{d}(q^2)}{\mathcal{D}(q^2)} \simeq \frac{\alpha_T(q^2)}{q^2 [1 - L(q^2, \zeta^2)F(q^2, \zeta^2)]^2} \frac{m_0^2 \Delta_F(0, \zeta^2)}{\Delta_F(q^2, \zeta^2)}$$

$$= \alpha_T(\zeta^2) \frac{F(q^2, \zeta^2)}{[1 - L(q^2, \zeta^2)F(q^2, \zeta^2)]^2} \Delta_F(0, \zeta^2) m_0^2$$

The IR running of the PI effective charge with momenta only depends on:

- The ghost dressing function
- The PT-BFM function L



PI-effective charge from lattice data with Nf=3 flavors at the physical point

Preliminary results:

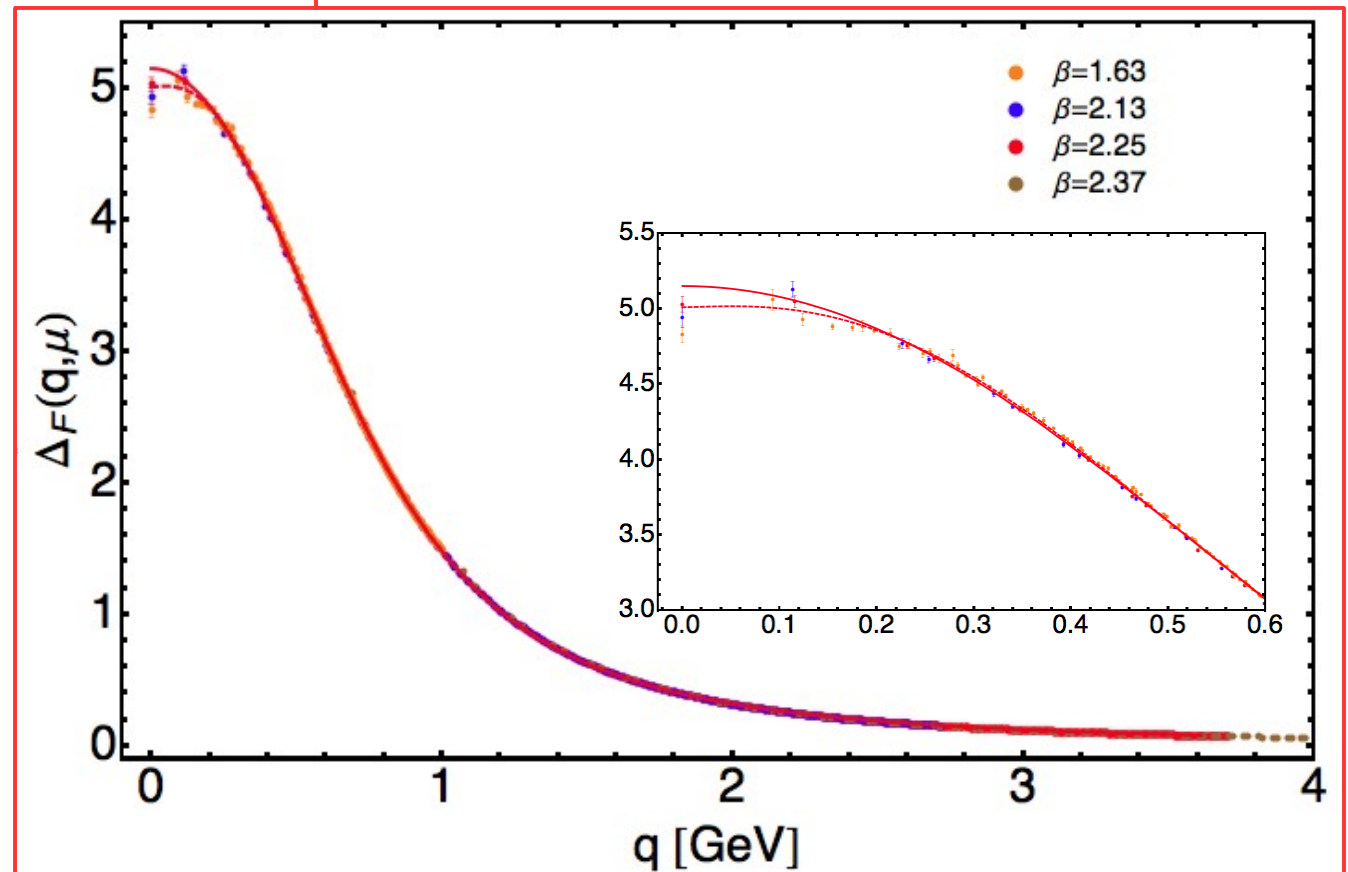
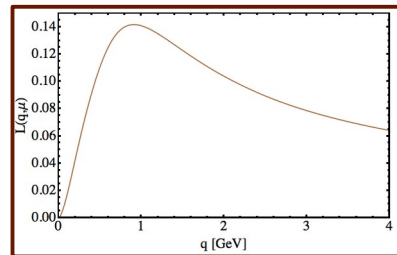
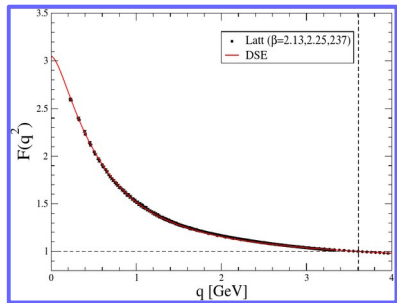
$$\hat{\alpha}_{\text{PI}}(q^2) = \frac{\hat{d}(q^2)}{\mathcal{D}(q^2)} \simeq \frac{\alpha_T(q^2)}{q^2 [1 - L(q^2, \zeta^2)F(q^2, \zeta^2)]^2} \frac{m_0^2 \Delta_F(0, \zeta^2)}{\Delta_F(q^2, \zeta^2)}$$

$$= \alpha_T(\zeta^2) \frac{F(q^2, \zeta^2)}{[1 - L(q^2, \zeta^2)F(q^2, \zeta^2)]^2} \Delta_F(0, \zeta^2) m_0^2$$

The IR running of the PI effective charge with momenta only depends on:

- The ghost dressing function
- The PT-BFM function L

Its strength depends also on the saturation point at zero-momentum of the gluon propagator



PI-effective charge from lattice data with Nf=3 flavors at the physical point

Preliminary results:

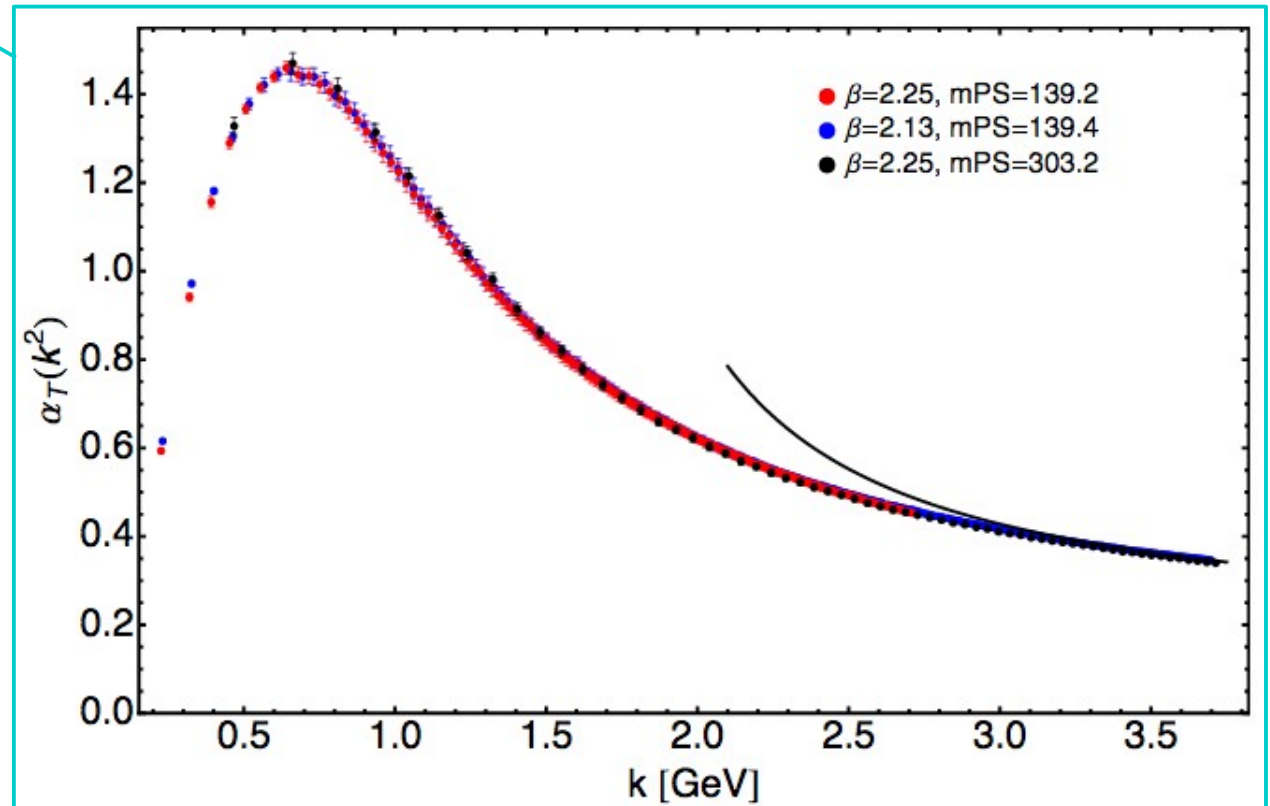
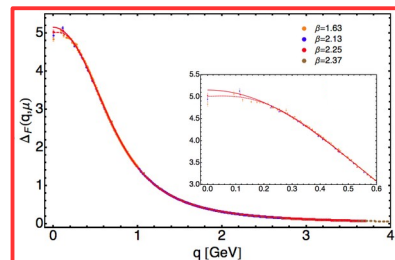
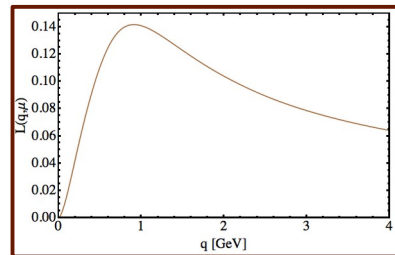
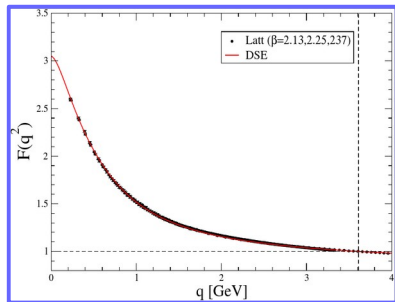
$$\hat{\alpha}_{\text{PI}}(q^2) = \frac{\hat{d}(q^2)}{\mathcal{D}(q^2)} \simeq \frac{\alpha_T(q^2)}{q^2 [1 - L(q^2, \zeta^2)F(q^2, \zeta^2)]^2} \frac{m_0^2 \Delta_F(0, \zeta^2)}{\Delta_F(q^2, \zeta^2)}$$

$$= \alpha_T(\zeta^2) \frac{F(q^2, \zeta^2)}{[1 - L(q^2, \zeta^2)F(q^2, \zeta^2)]^2} \Delta_F(0, \zeta^2) m_0^2$$

The IR running of the PI effective charge with momenta only depends on:

- The ghost dressing function
- The PT-BFM function L

Its strength depends also on the saturation point at zero-momentum of the gluon propagator and on the Taylor coupling.



PI-effective charge from lattice data with Nf=3 flavors at the physical point

Preliminary results:

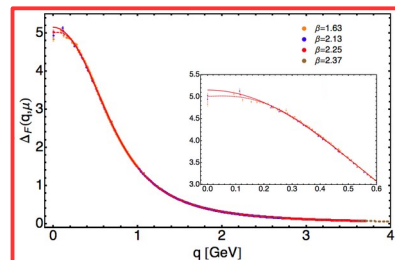
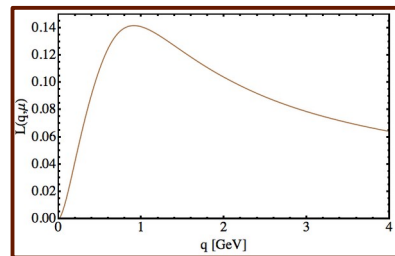
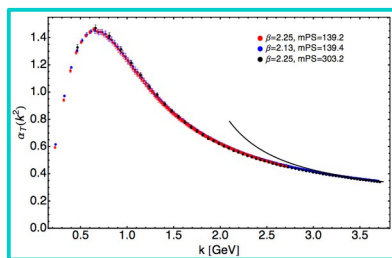
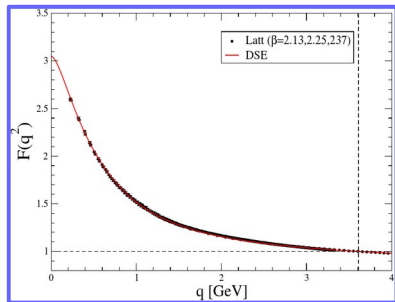
$$\hat{\alpha}_{\text{PI}}(q^2) = \frac{\hat{d}(q^2)}{\mathcal{D}(q^2)} \simeq \frac{\alpha_T(q^2)}{q^2 [1 - L(q^2, \zeta^2)F(q^2, \zeta^2)]^2} \frac{m_0^2 \Delta_F(0, \zeta^2)}{\Delta_F(q^2, \zeta^2)}$$

$$= \alpha_T(\zeta^2) \frac{F(q^2, \zeta^2)}{[1 - L(q^2, \zeta^2)F(q^2, \zeta^2)]^2} \Delta_F(0, \zeta^2) m_0^2$$

The IR running of the PI effective charge with momenta only depends on:

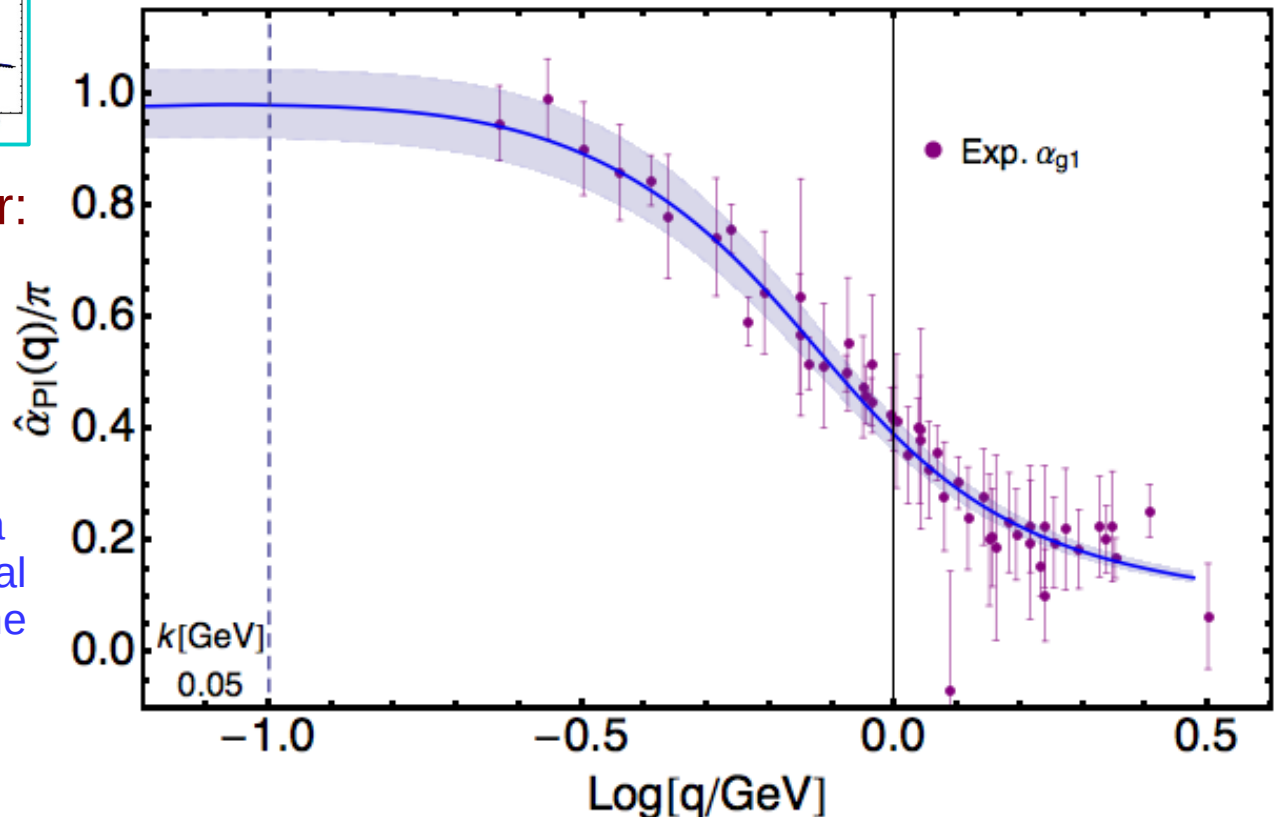
- The ghost dressing function
- The PT-BFM function L

Its strength depends also on the saturation point at zero-momentum of the gluon propagator and on the Taylor coupling.



All put together:

Less uncertainties (that of the gluon mass is only left here) and still a better agreement with the world data for the experimental determination of the Bjorken sum-rule effective charge.



Pion realistic picture: DGLAP evolution

Let us also consider the singlet components:
(an almost textbook exercise)

$$\gamma_{0,AB}^{S,(m)} = - \int_0^1 dx x^m P_{0,AB}^S(x)$$

$$\zeta^2 \frac{d}{d\zeta^2} \begin{pmatrix} M_q^{(m)}(\zeta) \\ M_G^{(m)}(\zeta) \end{pmatrix} = - \frac{\alpha(\zeta^2)}{4\pi} \underbrace{\begin{pmatrix} \gamma_{0,qq}^{S,(m)} & 2n_f \gamma_{0,qG}^{S,(m)} \\ \gamma_{0,Gq}^{S,(m)} & \gamma_{0,GG}^{S,(m)} \end{pmatrix}}_{\Gamma_0^{S,(m)}} \begin{pmatrix} M_q^{(m)}(\zeta) \\ M_G^{(m)}(\zeta) \end{pmatrix}$$

$$P^{-1} \Gamma_0^{S,(m)} P = \underbrace{\begin{pmatrix} \lambda_+^{(m)} & 0 \\ 0 & \lambda_-^{(m)} \end{pmatrix}}_{\Gamma_D^{(m)}}$$

Pion realistic picture: DGLAP evolution

Let us also consider the singlet components:
(an almost textbook exercise)

$$\gamma_{0,AB}^{S,(m)} = - \int_0^1 dx x^m P_{0,AB}^S(x)$$

$$\zeta^2 \frac{d}{d\zeta^2} P^{-1} \begin{pmatrix} M_q^{(m)}(\zeta) \\ M_G^{(m)}(\zeta) \end{pmatrix} = - \frac{\alpha(\zeta^2)}{4\pi} \Gamma_D^{(m)} P^{-1} \begin{pmatrix} M_q^{(m)}(\zeta) \\ M_G^{(m)}(\zeta) \end{pmatrix}$$

$$P^{-1} \Gamma_0^{S,(m)} P = \begin{pmatrix} \lambda_+^{(m)} & 0 \\ 0 & \lambda_-^{(m)} \end{pmatrix}$$



Pion realistic picture: DGLAP evolution

Let us also consider the singlet components:
(an almost textbook exercise)

$$\gamma_{0,AB}^{S,(m)} = - \int_0^1 dx x^m P_{0,AB}^S(x)$$

$$\zeta^2 \frac{d}{d\zeta^2} P^{-1} \begin{pmatrix} M_q^{(m)}(\zeta) \\ M_G^{(m)}(\zeta) \end{pmatrix} = -\frac{\alpha(\zeta^2)}{4\pi} \Gamma_D^{(m)} P^{-1} \begin{pmatrix} M_q^{(m)}(\zeta_H) \\ 0 \end{pmatrix}$$

$$P^{-1} \Gamma_0^{S,(m)} P = \begin{pmatrix} \lambda_+^{(m)} & 0 \\ 0 & \lambda_-^{(m)} \end{pmatrix}$$

Initial conditions at the hadronic scale, where only valence-quarks are assumed to be the correct degrees-of-freedom

Pion realistic picture: DGLAP evolution

Let us also consider the singlet components:
(an almost textbook exercise)

$$\gamma_{0,AB}^{S,(m)} = - \int_0^1 dx x^m P_{0,AB}^S(x)$$

$$\zeta^2 \frac{d}{d\zeta^2} P^{-1} \begin{pmatrix} M_q^{(m)}(\zeta) \\ M_G^{(m)}(\zeta) \end{pmatrix} = - \frac{\alpha(\zeta^2)}{4\pi} \Gamma_D^{(m)} P^{-1} \begin{pmatrix} M_q^{(m)}(\zeta_H) \\ 0 \end{pmatrix}$$

$$P^{-1} \Gamma_0^{S,(m)} P = \begin{pmatrix} \lambda_+^{(m)} & 0 \\ 0 & \lambda_-^{(m)} \end{pmatrix}$$

Initial conditions at the hadronic scale, where only valence-quarks are assumed to be the correct degrees-of-freedom, can be evolved and shown to produce non-zero gluon and sea-quark components.

$$P^{-1} \begin{pmatrix} M_q^{(m)}(\zeta) \\ M_G^{(m)}(\zeta) \end{pmatrix} = \exp \left(-\Gamma_D^{(m)} \int_{\ln \zeta_H^2}^{\ln \zeta^2} d \ln z^2 \frac{\alpha(z^2)}{4\pi} \right) P^{-1} \begin{pmatrix} M_q^{(m)}(\zeta_H) \\ 0 \end{pmatrix}$$

Pion realistic picture: DGLAP evolution

Let us also consider the singlet components:
(an almost textbook exercise)

$$\gamma_{0,AB}^{S,(m)} = - \int_0^1 dx x^m P_{0,AB}^S(x)$$

$$\begin{pmatrix} w_{11} & w_{12} \\ w_{21} & w_{22} \end{pmatrix} \zeta^2 \frac{d}{d\zeta^2} P^{-1} \begin{pmatrix} M_q^{(m)}(\zeta) \\ M_G^{(m)}(\zeta) \end{pmatrix} = -\frac{\alpha(\zeta^2)}{4\pi} \Gamma_D^{(m)} P^{-1} \begin{pmatrix} M_q^{(m)}(\zeta_H) \\ 0 \end{pmatrix}$$

$$P^{-1} \Gamma_0^{S,(m)} P = \begin{pmatrix} \lambda_+^{(m)} & 0 \\ 0 & \lambda_-^{(m)} \end{pmatrix}$$

Initial conditions at the hadronic scale, where only valence-quarks are assumed to be the correct degrees-of-freedom, can be evolved and shown to produce non-zero gluon and sea-quark components.

$$M_q^{(m)}(\zeta) = M_q^{(m)}(\zeta_H) \times \left[\frac{w_{11}w_{22}}{\text{Det}(P)} \exp\left(-\frac{\lambda_+^{(m)}}{4\pi} \int_{\ln \zeta_H^2}^{\ln \zeta^2} dt \alpha(t)\right) - \frac{w_{12}w_{21}}{\text{Det}(P)} \exp\left(-\frac{\lambda_-^{(m)}}{4\pi} \int_{\ln \zeta_H^2}^{\ln \zeta^2} dt \alpha(t)\right) \right]$$

$$M_G^{(m)}(\zeta) = M_q^{(m)}(\zeta_H) \frac{w_{22}w_{21}}{\text{Det}(P)} \times \left[\exp\left(-\frac{\lambda_+^{(m)}}{4\pi} \int_{\ln \zeta_H^2}^{\ln \zeta^2} dt \alpha(t)\right) - \exp\left(-\frac{\lambda_-^{(m)}}{4\pi} \int_{\ln \zeta_H^2}^{\ln \zeta^2} dt \alpha(t)\right) \right]$$

Pion realistic picture: DGLAP evolution

Let us also consider the singlet components:
(an almost textbook exercise)

$$\gamma_{0,AB}^{S,(m)} = - \int_0^1 dx x^m P_{0,AB}^S(x)$$

$$\begin{pmatrix} 1 & 3/4 \\ -1 & 1 \end{pmatrix} \zeta^2 \frac{d}{d\zeta^2} P^{-1} \begin{pmatrix} M_q^{(m)}(\zeta) \\ M_G^{(m)}(\zeta) \end{pmatrix} = -\frac{\alpha(\zeta^2)}{4\pi} \Gamma_D^{(m)} P^{-1} \begin{pmatrix} M_q^{(m)}(\zeta_H) \\ 0 \end{pmatrix}$$

$$P^{-1} \Gamma_0^{S,(1)} P = \begin{pmatrix} 56/9 & 0 \\ 0 & 0 \end{pmatrix}$$

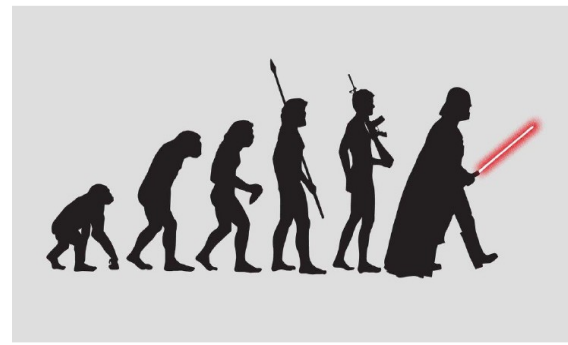
Case m=1

Initial conditions at the hadronic scale, where only valence-quarks are assumed to be the correct degrees-of-freedom, can be evolved and shown to produce non-zero gluon and sea-quark components.

$$M_q^{(1)}(\zeta) = M_q^{(1)}(\zeta_H) \left[\frac{3}{7} + \frac{4}{7} \exp \left(-\frac{56}{36\pi} \int_{\ln \zeta_H^2}^{\ln \zeta^2} dt \alpha(t) \right) \right]$$

$$M_G^{(1)}(\zeta) = \frac{4}{7} M_q^{(1)}(\zeta_H) \left[1 - \exp \left(-\frac{56}{36\pi} \int_{\ln \zeta_H^2}^{\ln \zeta^2} dt \alpha(t) \right) \right]$$

PDA and LFWF evolution



Standard PDA evolution:

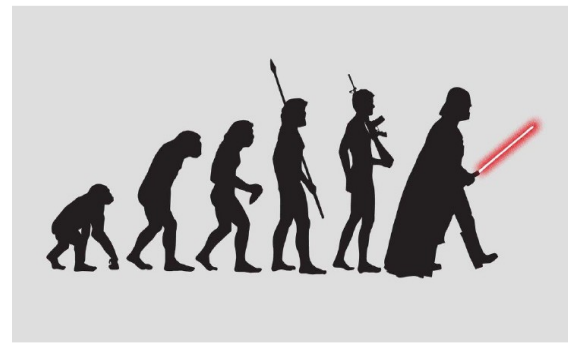
- We project **PDA** onto a 3/2-Gegenbauer polynomial basis. Such that it **evolves**, from an initial scale ζ_0 to a final scale ζ , **according to** the corresponding **ERBL equations**:

$$\phi(x; \zeta) = 6x(1-x) \left[1 + \sum_{n=1} a_n(\zeta) C_n^{3/2}(2x-1) \right],$$

$$a_n(\zeta) = a_n(\zeta_0) \left[\frac{\alpha(\zeta^2)}{\alpha(\zeta_0^2)} \right]^{\gamma_0^n / \beta_0}, \quad \gamma_0^n = -\frac{4}{3} \left[3 + \frac{2}{(n+1)(n+2)} - 4 \sum_{k=1}^{n+1} \frac{1}{k} \right].$$

- Thus, any PDA at hadronic scale evolves logarithmically towards its conformal distribution, $\phi(x)=6x(1-x)$.
 - Quark mass and flavor become irrelevant. Broad PDA becomes narrower, skewed PDA becomes symmetric.

PDA and LFWF evolution



LFWF evolution:

$$\phi(x) = \frac{1}{16\pi^3} \int d^2\vec{k}_\perp \psi^{\uparrow\downarrow}(x, k_\perp^2)$$

- We look for a way to evolve the LFWF.
- First, let's assume that the LFWF admits a similar Gegenbauer expansion. That is:

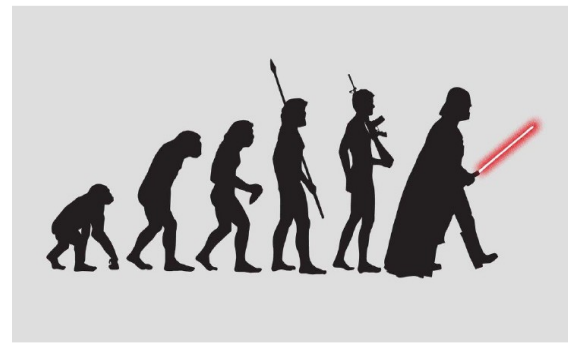
$$\psi(x, k_\perp^2; \zeta) = 6x(1-x) \left[\sum_{n=0} b_n(k_\perp^2; \zeta) C_n^{3/2}(2x-1) \right],$$

$$a_n(\zeta) = \frac{1}{16\pi^3} \int d^2\vec{k}_\perp b_n(k_\perp^2; \zeta) \text{ (for } n \geq 1), \quad \frac{1}{16\pi^3} \int d^2\vec{k}_\perp b_0(k_\perp^2; \zeta) = 1.$$

- 1-loop ERBL evolution of $a_n(\zeta)$ implies:

$$\frac{1}{a_n(\zeta)} \frac{d}{d \ln \zeta^2} a_n(\zeta) = \frac{\int d^2\vec{k}_\perp \frac{d}{d \ln \zeta^2} b_n(k_\perp^2; \zeta)}{\int d^2\vec{k}_\perp b_n(k_\perp^2; \zeta)},$$

PDA and LFWF evolution



LFWF evolution:

$$\phi(x) = \frac{1}{16\pi^3} \int d^2\vec{k}_\perp \psi^{\uparrow\downarrow}(x, k_\perp^2)$$

- Now, if we take a factorization assumption, we arrive at:

$$\frac{b_n(k_\perp^2; \zeta)}{b_n(k_\perp^2; \zeta_0)} = \frac{\hat{b}_n(\zeta)}{\hat{b}_n(\zeta_0)} = \left[\frac{\alpha(\zeta^2)}{\alpha(\zeta_0^2)} \right]^{\gamma_0^n / \beta_0}, \quad b_n(k_\perp^2; \zeta) \equiv \hat{b}_n(\zeta) \chi_n(k_\perp^2).$$

- Supplemented by the condition $\chi_n(k_\perp^2) \equiv \chi(k_\perp^2)$, one gets $\hat{b}_n(\zeta) \equiv a_n(\zeta)$.
- Such that, the following factorised form is obtained:

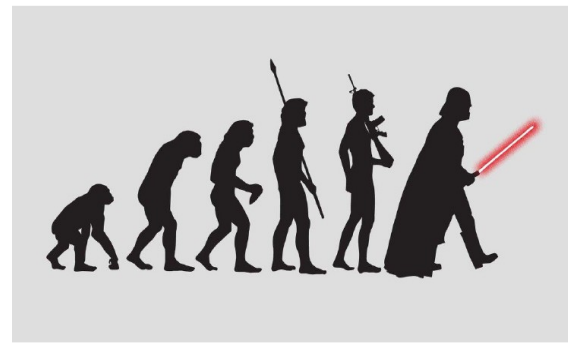
$$\psi(x, k_\perp^2; \zeta) \equiv \phi(x; \zeta) \chi(k_\perp^2) \longrightarrow \text{LFWF Evolves like PDA}$$

- Which is far from being a general result, but an useful approximation instead.

PDA and LFWF evolution

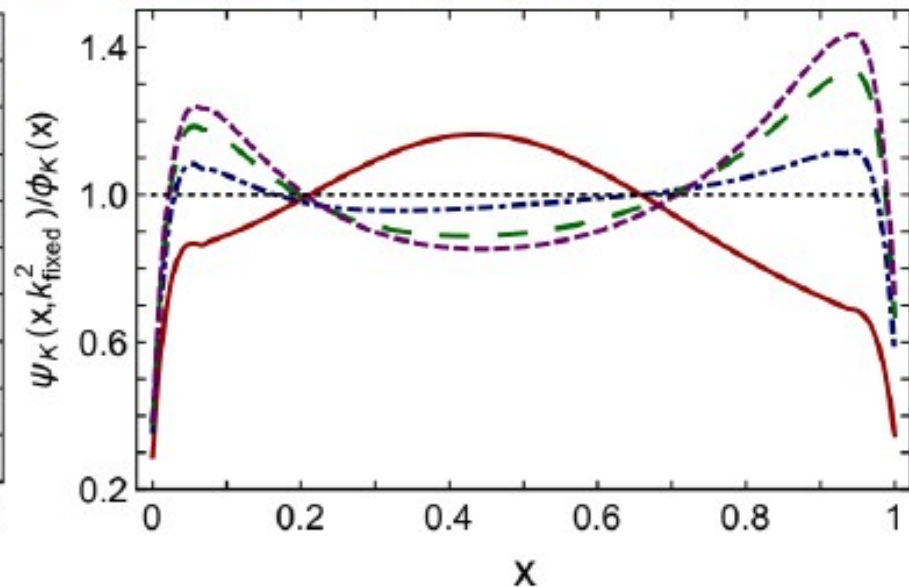
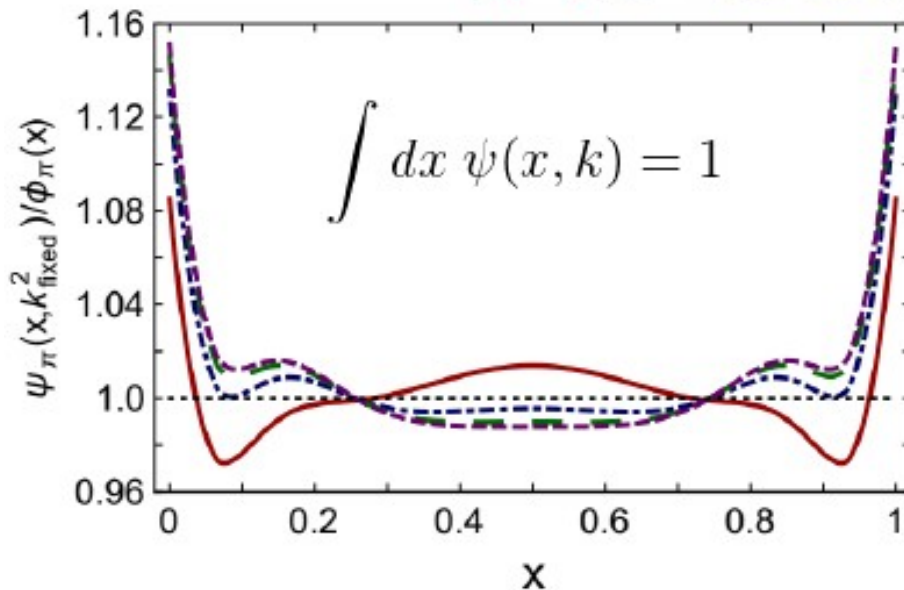
Testing the factorization ansatz:

$$\psi(x, k_{\perp}^2; \zeta) \equiv \phi(x; \zeta) \chi(k_{\perp}^2)$$



- A first validation of the factorized ansatz is addressed in **Phys.Rev. D97 (2018) no.9, 094014**:

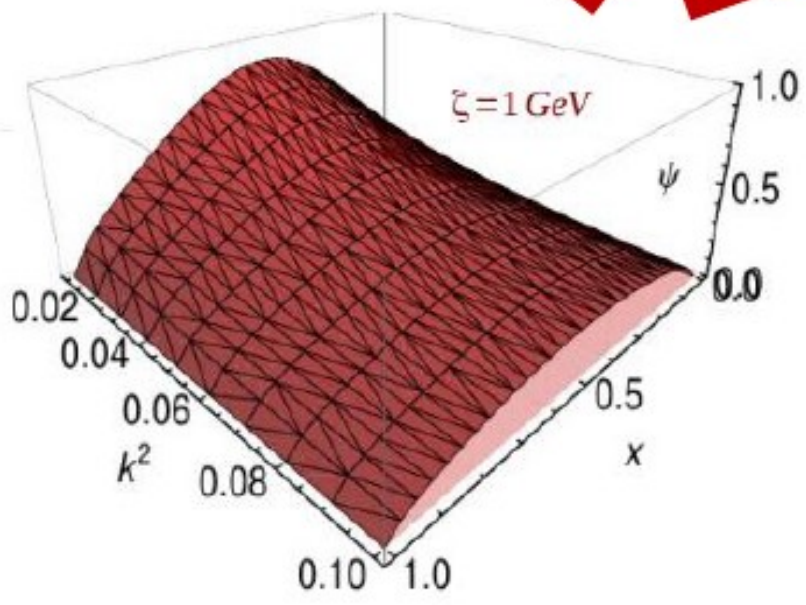
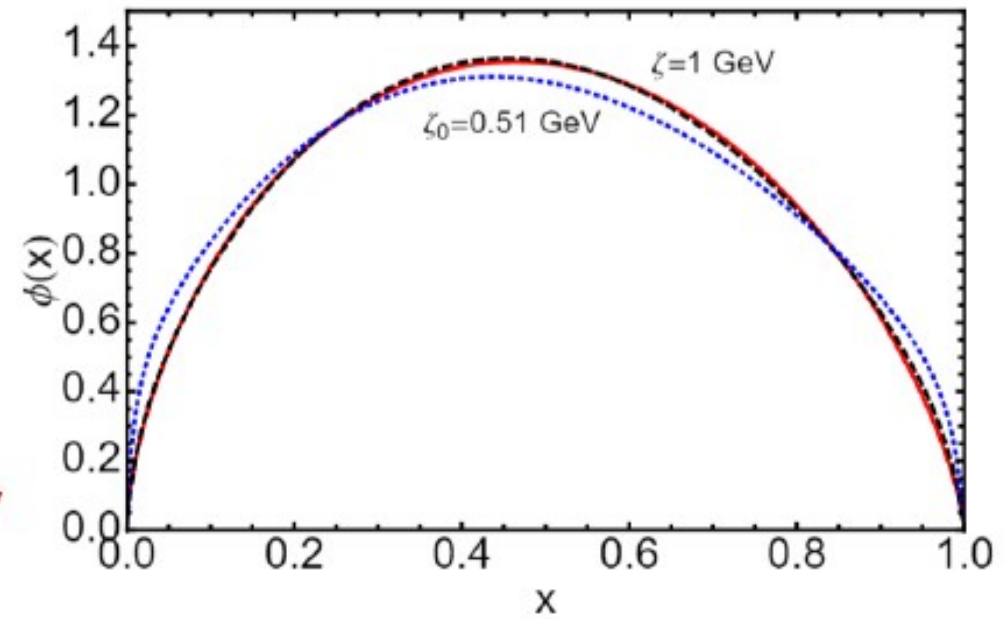
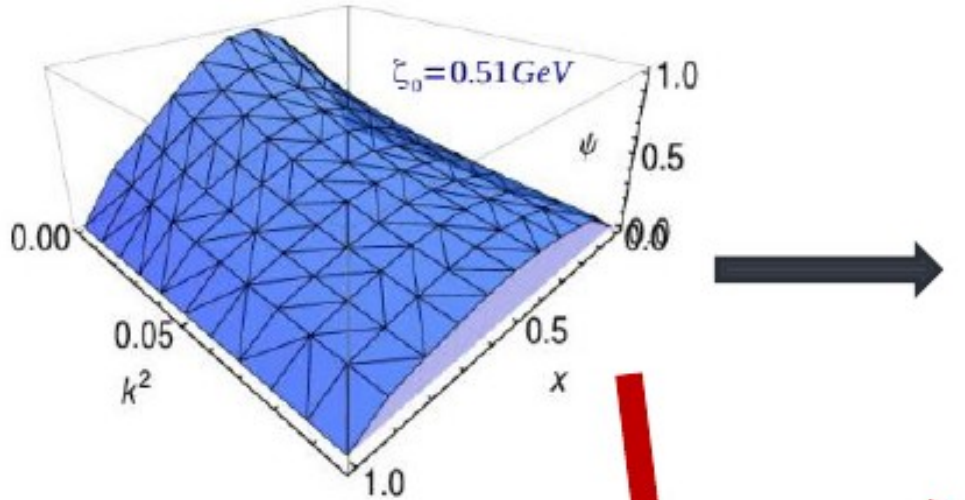
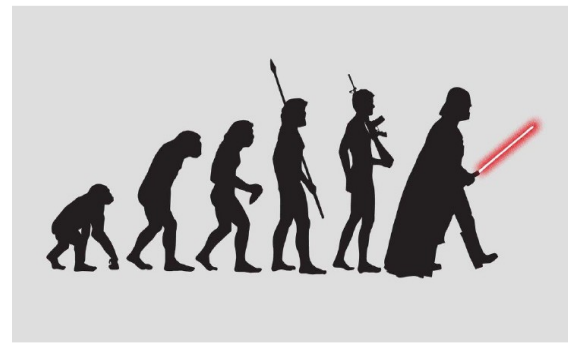
$k^2=0$, $k^2=0.2$ GeV, $k^2=0.8$ GeV, $k^2=3.2$ GeV



- If the factorized ansatz is a good approximation, then the plotted ratio must be 1. For the pion, it slightly deviates from 1; for the kaon, the deviation is much larger.

PDA and LFWF evolution

Testing the factorization ansatz:

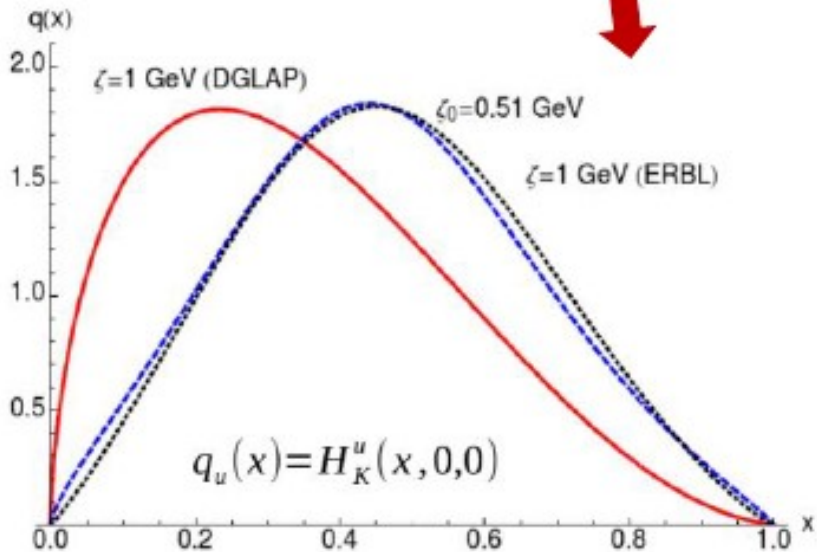
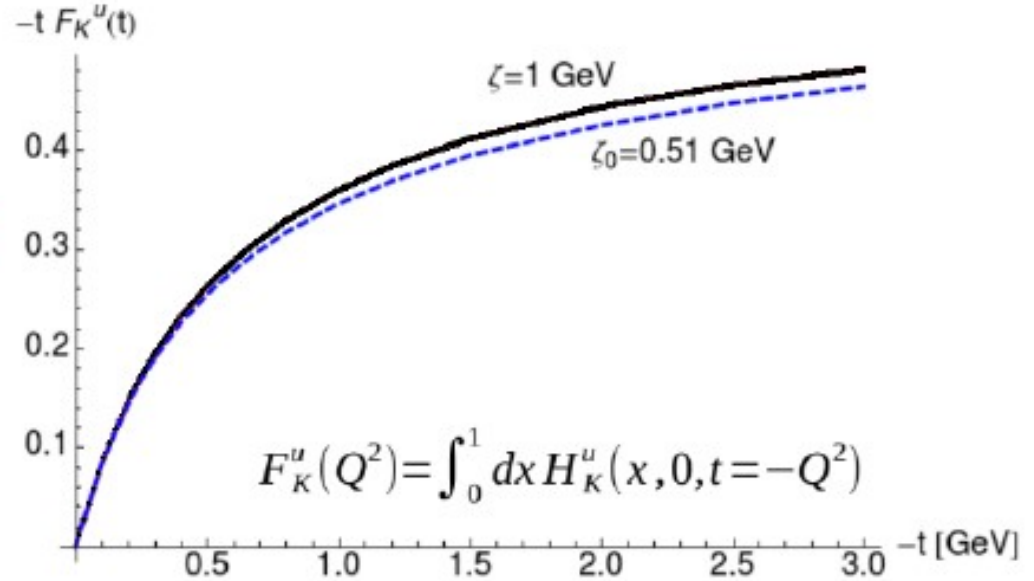
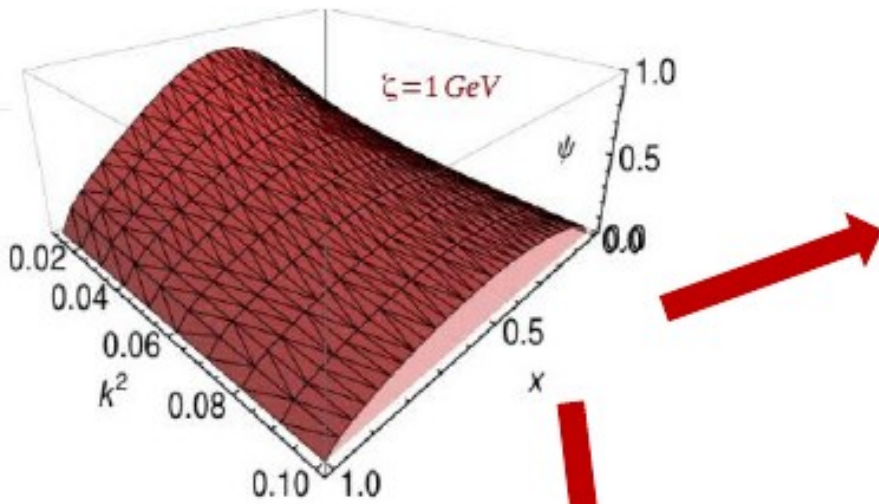
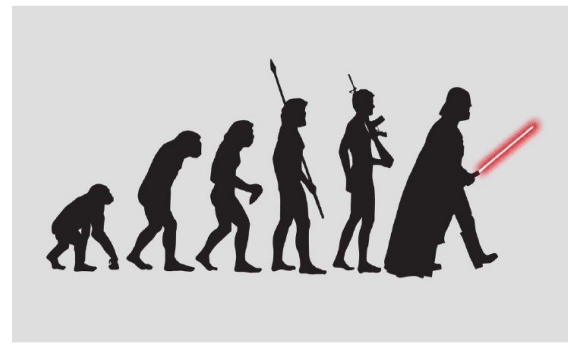


- 1) Compute LFWF and ERBL running of PDA
- 2) ERBL running of LFWF and compute PDA

Notably, 1) and 2) are **equivalent**. Factorization assumption and evolution seem reasonable.

PDA and LFWF evolution

How ERBL and DGLAP evolutions make contact:

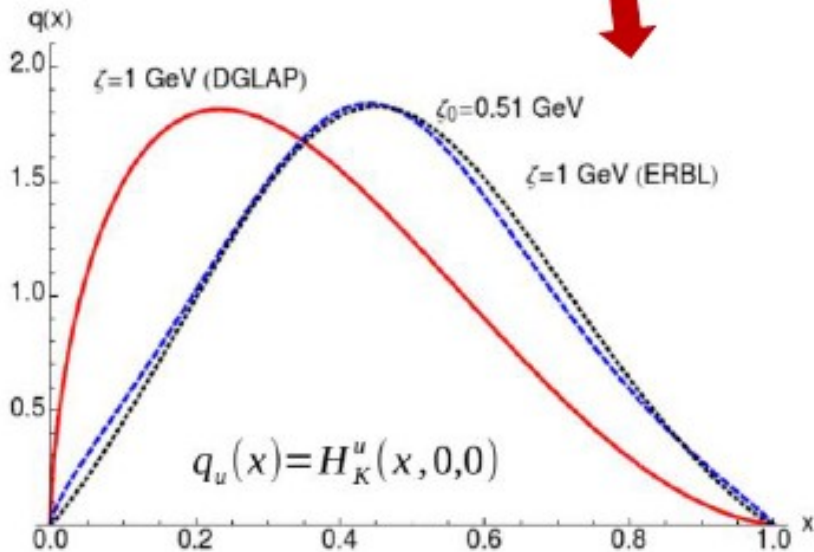
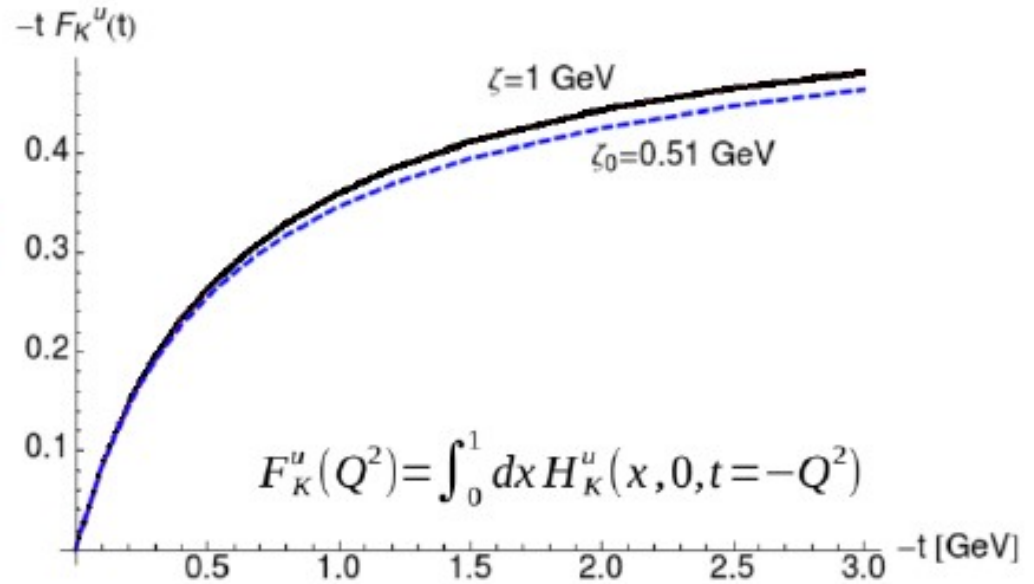
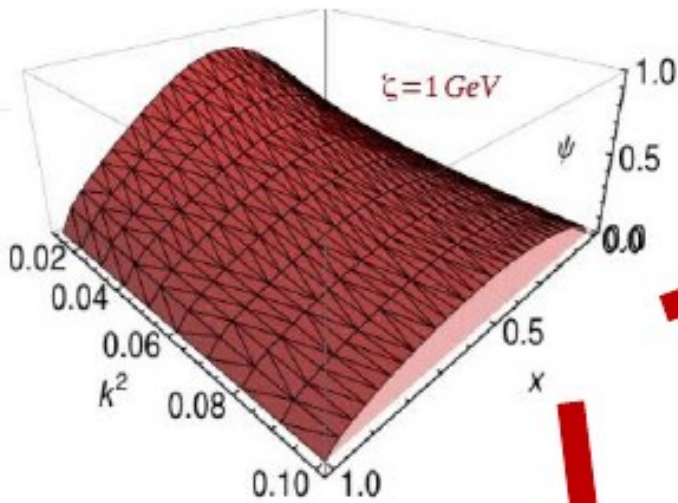
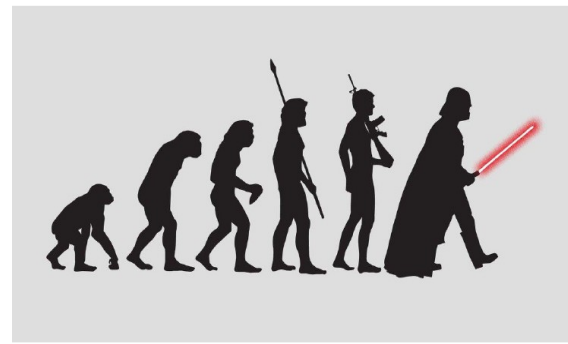


- 1) Obtained from ERBL evolution of LFWF
- 2) Obtained from DGLAP evolution of GPD

Clearly, 1) and 2) are not equivalent.

PDA and LFWF evolution

How ERBL and DGLAP evolutions make contact:



- 1) Obtained from ERBL evolution of LFWF
- 2) Obtained from DGLAP evolution of GPD

Clearly, 1) and 2) are **not equivalent**.

Sea-quark and gluon content incorporated to the parton distribution by DGLAP are obviously not present in the valence-quark PDF from LFWFs!!!